Food & Function

ROYAL SOCIETY OF CHEMISTRY

PAPER

View Article Online
View Journal | View Issue

Cite this: *Food Funct.*, 2025, **16**, 3439

A type 4 resistant potato starch alters the cecal microbiome, gene expression and resistance to colitis in mice fed a Western diet based on NHANES data†

Elizabeth A. Pletsch, Harry D. Dawson, Lumei Cheung, Jack S. Ragonese, Celine T. Chen and Allen D. Smith *

Four major types of resistant starch (RS1–4) are present in foods and can be fermented to produce short-chain fatty acids (SCFAs), alter the microbiome and modulate post-prandial glucose metabolism. While studies in rodents have examined the effects of RS4 consumption on the microbiome, fewer have examined its effect on gene expression in the cecum or colon or resistance to bacterial-induced colitis, and those that have, use diets that do not reflect what is typically consumed by humans. Here we fed mice a Total Western Diet (TWD), based on National Health and Nutrition Examination Survey (NHANES) data for 6–7 weeks and then supplemented their diet with 0, 2, 5, or 10% of the RS4, Versafibe 1490™ (VF), a phosphorylated and cross-linked potato starch. After three weeks, mice were infected with *Citrobacter rodentium* (*Cr*) to induce colitis. Infected mice fed the 10% VF diet had the highest levels of *Cr* fecal excretion at days 4, 7 and 11 post-infection. Infected mice fed the 5% and 10%VF diets had increased hyperplasia and colonic damage compared with the control. Changes in bacterial genera relative abundance, and alpha and beta diversity due to diet were most evident in mice fed 10% VF. *Cr* infection also resulted in specific changes to the microbiome and gene expression both in the cecum and the colon compared with diet alone, including the expression of multiple antimicrobial genes, *Reg3b*, *Reg3g*, *NOS2* and *Ifng*. These results demonstrate that VF, a RS4, alters cecal and colonic gene expression, the microbiome composition and resistance to bacterial-induced colitis.

Received 25th September 2024,
Accepted 3rd March 2025

DOI: 10.1039/d4fo04697h

rsc.li/food-function

Introduction

Resistant starch (RS) is considered a dietary fiber that is not degraded by digestive enzymes in the small intestine and can be classified into four major types (RS1–4) based upon their physical and chemical properties.[1] Although consumption of 15–20 g d^{-1} of RS is recommended, most people consuming a Western diet average 4.9 g day^{-1}.[1,2] Consumption of fiber and RS can alter the microbiome and bacterial fermentation, including changes to SCFA production in the cecum and colon in rodents,[3–6] pigs[7–9] and humans[10,11] that have been linked to health benefits.[12] There is mounting evidence that different fibers and RS differentially alter microbial composition and bacterial metabolites.[13,14] Furthermore, the structural complexity of the fiber can influence the degree of changes to the microbiome.[15] Interestingly, members of the same RS or fiber type can have differential effects on the microbiome and bacterial metabolites.[16,17] These differences are likely due to variations in their fine structure that may favor the growth of certain bacterial strains over others.[17–19]

Multiple rodent studies have looked at the effect of RS consumption in mice fed a "Western" high-fat diet.[20–23] In general, these studies used modified AIN-93 diets with 45–60% of the calories coming from lard or milkfat and 8–19% from sucrose; however, the diets used in these studies do not reflect what is typically consumed in an American diet. To address this, we and others[24–26] have used the Total Western Diet (TWD), developed using the 50th percentile daily intake levels for macro and micronutrients from NHANES, including fewer calories from protein and carbohydrates, double the fat with more saturated and monounsaturated fats, less polyunsaturated fat, fewer complex carbohydrates, and twice the level of simple sugars compared with the AIN-93 diet.[27] Thus, our studies using the TWD as our basal diet for studies examining the effect of added dietary RS on the micro-

Diet, Genomics, and Immunology Laboratory, Beltsville Human Nutrition Research Center, Agricultural Research Service, United States Department of Agriculture, Rm. 228, Bldg. 307C, BARC-East, 10300 Baltimore Ave., Beltsville, MD, 20705, USA. E-mail: allen.smith@usda.gov; Tel: +(301) 504-8577 ext. 280

†Electronic supplementary information (ESI) available: Supplemental Fig. 1–4 and Tables 1–12. See DOI: https://doi.org/10.1039/d4fo04697h

biome and host physiological responses represent a novel, more relevant approach.

Ulcerative colitis is an inflammatory disease of the gastrointestinal tract of unknown etiology[28] that can cause significant morbidity, disrupting quality of life[29] and is known to be influenced by the microbiome.[30] Bacterial infections can also cause colitis including those caused by Enteropathogenic (EPEC) and Enterohemorrhagic *Escherichia coli* (EHEC).[31] *Citrobacter rodentium* (*Cr*) is an *Escherichia coli*-like bacterium that naturally infects mice. It shares 67% of its genes with EPEC and EHEC, including genes important for pathogenicity and virulence.[32] *Cr* causes disease analogous to enteropathogenic bacterial infections in humans and serves as a useful model to study infectious colitis.[32–34]

Several studies have looked at the effect of fiber and/or a high-fat diet on *Cr* infections. Feeding a lard-based semi-purified Western-style diet altered the microbiome and impeded colonization and clearance of *Cr.*[35] Feeding ground flaxseed reversed the protective effect of a low-fat diet on a *Cr* infection but this was not observed in mice fed a high-fat diet.[36] The lipid content of a high-fat diet rather than total calories impacted *Cr* pathogen load and colonic pathology.[37] *Cr*-infected mice fed a fiber-deficient diet had increased pathology and lethality.[38,39] Mice fed an AIN-93G diet containing either wheat bran or a type 2 resistant corn starch alone or in combination with a *Cr* infection significantly altered microbiome and reduced colitis severity due to *Cr* infection.[40] The effect of short-chain fatty acids (SCFAs), bacterial fermentation products such as butyrate, on *Cr* infection has also been studied, showing that administration of butyrate enemas altered the microbiome and reduced *Cr*-induced colitis.[41] Recent work has shown that even within the same strain of mice susceptibility to *Cr* can vary, is microbiome dependent,[42] and that resistance was associated with a microbiome that produced increased levels of butyrate. Dietary carbohydrates, including different fibers and RS, can also affect immune cells including binding to TLR-2, TLR-5 and other receptors (reviewed in ref. 43). Together, these studies suggest that fermentable substrates can influence the outcome of *Cr* infections possibly by altering the microbiome, bacterial metabolites and intestinal gene expression.

The addition of RS2 and chemical modified RS4 starches not normally found in nature has become popular in food additives as their addition increases fiber content. Certain RS2, native starches, and RS4, chemically modified starches, have been shown to improve insulin sensitivity in mice[44] and differentially impact the gut microbiome in humans;[45] however, fewer studies have investigated their effect on bacterial-induced colitis. In a previous study, we demonstrated that the addition of a RS2 potato starch (RPS, PenPure 10, Ingredion) to the TWD induced significant changes to the intestinal microbiome and transcriptome.[46] Unexpectedly, we found that higher levels of RPS (10%) increased the efficiency of infection and colon pathology induced by *Cr.*[47] However, it is unknown what the effect of chemically modifying a RS will have on its ability to affect a *Cr* infection. To investigate this, we conducted studies examining the effect of feeding a Western-style diet based on NHANES data containing different levels of Versafibe 1490™ (VF), a phosphorylated and crosslinked potato starch, on subsequent *Cr* infections.

Materials and methods

Animals and diet

C57BL/6NCr mice were originally obtained from Charles River (Frederick, MD) and were bred in-house. Mice were fed rodent chow (Teklad 2020X, Frederick, MD) and housed in ventilated filter-top cages at the USDA Beltsville Human Nutrition Research Center animal facility under 12 h light/dark cycle. Timed breedings were set up and offspring were weaned at 3–4 weeks of age. After weaning, female mice were group housed (4–5 per cage) and were fed the TWD (ESI Table 1†)[27] for 6–7 weeks. Mice were then divided into 4 dietary treatment groups and fed for an additional 3–4 weeks with the TWD or TWD supplemented with 2%, 5%, or 10% w/w VF (Ingredion, Westchester, IL), a phosphorylated and crosslinked potato starch that contains 85% fiber as measured by the AOAC 991.43 method (Ingredion Technical Specification sheet), substituted for an equivalent amount of corn starch.

Citrobacter rodentium infections

After feeding the TWD or VF diets for an additional three weeks, mice were infected with 2.5–5.0 × 10^9 cfu of a nalidixic acid-resistant mutant of the *Cr* strain DBS100 (ATCC 51459) as described previously.[47] Uninfected controls received LB broth. All animal procedures were performed in accordance with the Guidelines for Care and Use of Laboratory Animals and approved by the USDA/ARS Beltsville Area Institutional Animal Care and Use Committee (Protocol 22-04).

Sample processing and analysis

Three experiments were conducted. For measurement of fecal *Cr* shedding on days 4, 7 and 11 post-infection (n = 15–29) and tissue to body weight ratios on mice euthanized (by a ketamine/xylazine overdose followed by exsanguination) at day 12 post-infection (n = 10–20 per group), data from three experiments were pooled. Samples from Experiment 3 were used for the gene expression, microbiome and histology measurements (n = 5–10 per group). After infection, mice were periodically weighed, and fecal pellets were collected to measure shedding of *Cr*. Fecal pellets were homogenized in LB broth and serial dilutions plated on LB agar plates containing 50 μg mL^{-1} nalidixic acid. Results were expressed as $\log_{10}$ cfu g^{-1} feces. Mice that were not productively infected as measured by low or no fecal load early in infection (day 4) were removed from all analyses to ensure uniform infection kinetics. Mice were euthanized on day 12 post-infection to obtain tissues and cecal contents for analyses. The colon was excised, the colonic contents removed, the terminal six cm of the colon was then taken, the tissue weighed and subdivided into one-centimeter portions that were fixed in 4% formalin for histology or snap frozen for

gene expression analysis. The cecum was excised, weighed and snap frozen for gene expression analysis, and cecal contents were collected for microbial analysis. The spleen was removed, weighed and snap frozen. Fecal pellets were weighed and homogenized in 10 volumes of water, centrifuged to remove debris and the pH of the supernatant measured.

Histology

Equivalent one cm sections from the distal colon (DC) were obtained on day 12 post-infection and fixed in buffered 4% paraformaldehyde. The sections were paraffin embedded and 5 μm sections were cut and stained with hematoxylin and eosin (H&E). The slides were coded, and sections were evaluated for damage to the surface epithelium (0–4), loss of crypt architecture (0–4), and the presence of an inflammatory cell infiltrate (0–4), maximum score of 12. Mucosal depth was measured using a Nikon Eclipse E800 microscope and Nikon NIS-Elements software V4.6. For each mouse, the mucosal depth was determined by averaging multiple measurements of well-oriented crypts and the average values were then used to determine statistical differences between dietary groups.

16S sequencing and analysis of cecal contents

DNA was isolated from cecal contents using a PowerFecal Pro Kit (Qiagen Germantown MD) following the manufacturer's instructions and was further purified using the DNA Clean and Concentration kit (Zymo, Irvine, CA). The DNA concentration of the samples was determined using the Quant-it PicoGreen dsDNA kit (Invitrogen, Waltham, MA). DNA was submitted to the Michigan State University RTSF Genomics Core for targeted amplicon library preparation and sequencing. The V4 hypervariable region of the 16S rRNA gene was amplified using dual-indexed, Illumina-compatible primers described in Kozich, J. J., *et al.* (2013).[48] PCR products were batch normalized using an Invitrogen SequalPrep DNA Normalization plate and product recovered from the plates pooled. The pool was concentrated and cleaned up using a QIAquick Spin column and AMPure XP magnetic beads. The pool was QC'd and quantified using a combination of Qubit dsDNA HS, Agilent 4200 TapeStation HS DNA1000 and Invitrogen Collibri Illumina Library Quantification qPCR assays. This pool was loaded onto one MiSeq v2 Standard flow cell and sequencing was carried out in a 2 × 250 bp paired end format using a MiSeq v2 500 cycle reagent cartridge. Custom sequencing and index primers complementary to the 515f/806r oligomers were added to appropriate wells of the reagent cartridge. Base calling was done by Illumina Real Time Analysis (RTA) v1.18.54 and output of RTA was demultiplexed and converted to FastQ format with Illumina Bcl2fastq v2.20.0. The FASTQ files with raw data were submitted to the National Center for Biotechnology Information (NCBI) Sequence Read Archive (SRA) under Bioproject number PRJNA1141498, GEO Accession: GSE273638.

The 16S rRNA tag data curation and processing were performed as previously reported[49] using the CLC Microbial Genomics Module (QIAGEN Bioinformatics, CLC Genomics Workbench version 23, Redwood City, CA) following its standard Operational Taxonomic Unit (OTU) clustering workflow with some modifications. Paired reads were first merged into contigs, followed by removal of the adapters, nucleotides below Q30, reads containing more than two ambiguous nucleotides or shorter than five. Samples were then filtered by removing reads below 150 bp or using the minimum 50% from the median times the median number of reads across all samples. The aligned contigs were mapped to the SILVA SSU database from release v138.1.[50] Chimeras were detected with *k*-mer search and removed from further processing and analysis. Sequences were then clustered into OTUs at 99% similarity and low abundance OTUs were filtered out. Alpha and beta diversity were estimated using OTUs aligned with the MUSCLE tool[51] to reconstruct the phylogenetic tree by a Maximum Likelihood approach. OTU count abundance was further collapsed into genus, family and phylum taxa levels for downstream analysis. Hierarchical clustering and principal coordinates analysis (PCoA) were performed with the OTU or taxon-specific abundance profiles to examine changes induced by the VF treatments with and without infection and visualized using JMP Statistical Software (JMP12, JMP Statistical Discovery LLC, Cary, NC). To measure the effect size and significance of beta diversity, Permutational analysis of variance (PERMANOVA)[52] was done using *vegan*[53,54] (R, version 4.3.2, Boston, MA) followed by *pairwiseAdonis*[55] for pairwise comparisons. The differential abundance analysis for all taxa and OTUs was performed with the MaAslin2 or CLC Genomics and relative abundance heatmaps were generated using *pheatmap.*[56]

RNASeq analysis of cecum and distal colon tissue

RNA from the cecum and DC was isolated using Tri-Reagent (Zymo, Irvine, CA) and Purelink RNA kits (Invitrogen, Carlsbad, CA). The samples were further purified using RNA Clean and Concentrate columns (Zymo, Irvine, CA) and the samples were submitted to the Michigan State University RTSF Genomics Core facility for sequencing. Libraries were prepared using Illumina Stranded mRNA Prep, Ligation kit with IDT for Illumina Unique Dual Indexes following the manufacturer's recommendations. Completed libraries were quantified using a combination of Qubit dsDNA HS and Agilent 4200 TapeStation HS DNA1000 assays. Libraries were pooled in equimolar amounts for multiplexed sequencing, and the pool quantified using the Invitrogen Collibri Quantification qPCR kit.

The pools were loaded onto an Illumina NovaSeq S2 flow cell and sequencing was performed in 1 × 100 bp single read format using a NovaSeq 6000 v1.5 100 cycle reagent kit. Base calling was done by Illumina Real Time Analysis (RTA) v3.4.4 and output of RTA was demultiplexed and converted to FastQ format with Illumina Bcl2fastq v2.20.0. The FASTQ files with raw data and the gene expression profiles were submitted to the National Center for Biotechnology Information (NCBI) Sequence Read Archive (SRA) under the BioProject ID: PRJNA1141498.

Correlation analyses

Correlations between bacterial relative abundance and gene expression were analyzed using Kendall's tau coefficient and FDR-adjusted *p*-values <0.05 using *corrtable* within Galaxy (**https://usegalaxy.eu**).[57] Due to the large number of comparisons, we only considered differentially abundant bacteria in cecum and upregulated DEGs in the host distal colon for analysis for each treatment comparing doses of VF in infected animals compared with the control. Significant positive correlations using a threshold of 0.8 and genes in Reactome pathway MMU-180215 Cytokine Signaling in Immune System, were used to establish correlation networks in Cytoscape v3.10.3.[58]

Statistical analyses

Data were analyzed using a Student's *t*-test, one-way or two-way ANOVA followed by the Holm–Sidak or Tukey Multiple Comparisons Procedure where applicable, were carried out using GraphPad Prism Software version 10.2.3 (GraphPad Software, Boston, MA) or SigmaPlot version 15.1 (Grafiti, Palo Alto, CA). Data were transformed as necessary to achieve equal variance and normality. In cases where equal variance and normality could not be met, a Welch's *t*-test or Mann–Whitney rank sum test or a Kruskal–Wallis one way analysis of variance on ranks was used. Fecal *Cr* loads and histopathology scores were analyzed by a Mann–Whitney rank sum test. Pairwise comparisons between treatments were conducted with the Student's *t*-test. For graphical purposes, the mean and SEM of untransformed data are shown. Transcriptomes were subjected to differential expression analysis with CLC Genome Workbench. Differentially expressed genes (DEGs) were determined to be genes that were up or down regulated ≥1.5-fold, respectively, at a false discovery rate (FDR)-adjusted *p* value of <0.05. We functionally annotated DEGs using our Porcine Translational Research Database.[59] The database serves to translate data found in rodents or pigs to human. VENN analysis of DEGs within individual groups was conducted using the online tool, VENNY 2.1 (**https://bioinfogp.cnb.csic.es/tools/venny/index.html**). Pathway analysis on DEGs was conducted using the online tool, DAVID (**https://david.ncifcrf.gov**)[60] using Knowledgebase v2022q2. Data were queried against the embedded Reactome[61] and KEGG database. VENN analysis was also conducted on differentially expressed (at an FDR-adjusted *p* value of <0.05%) Reactome and KEGG pathways identified by DAVID.

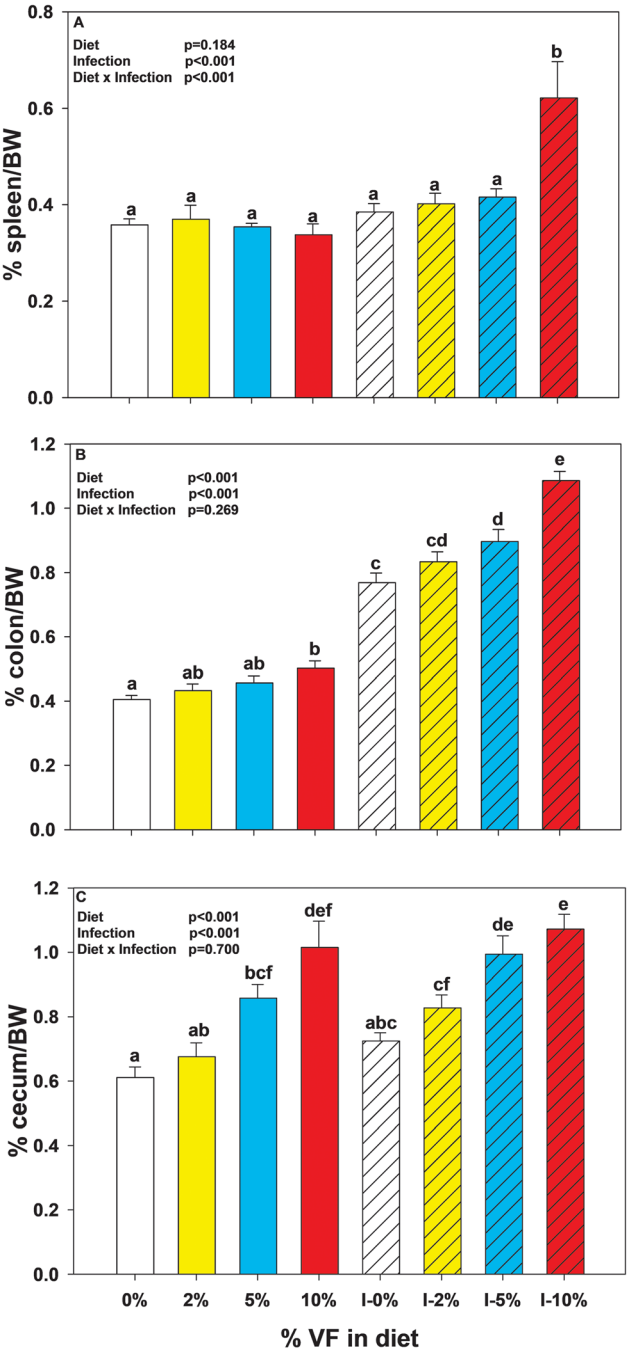

Fig. 1 Effect of VF consumption and *Cr* infection on percent tissue to body weight ratios. Percent tissue/body weight (BW) ratios of the (A) spleen, (B) distal colon, and (C) cecum in uninfected and *Cr*-infected mice. Results are shown as mean ± SEM and different letters indicate statistical significance at $p < 0.05$, $n = 10–20$ per group, pooled from three experiments.

Results

Effect of VF on tissue weights, fecal pH, and *Cr*-induced colitis

Body weights (BWs) were not affected by feeding VF or by infection with *Cr* (ESI Fig. 1A†). The effect of feeding VF and *Cr* infection on organ/BW ratios was determined at euthanasia. The %spleen/BW ratios were only increased in infected mice fed the 10% VF diet (Fig. 1A). The %colon/BW ratio increased with increasing dietary VF, but significance was achieved only in mice fed the 10% VF diet (Fig. 1B). The %colon/BW ratios in infected mice were higher than in uninfected mice at all VF doses which is indicative of the inflammatory response to infection that leads to hyperplasia and thickening of the colon tissue. In addition, infected mice fed the 5% and 10% VF diets had higher % colon/BW ratios than infected mice on the TWD.

Similarly, the % cecum/BW ratio was significantly increased in uninfected mice fed the 5% and 10% VF diets suggesting increased fermentation and/or accumulation of undigested material in mice consuming VF diets (Fig. 1C). Infection did not significantly alter the % cecum/BW ratio of mice fed the basal TWD compared with uninfected mice, but mice fed the 2% or 5% but not 10% VF diets did see an increased % cecum/BW ratio compared with their corresponding uninfected groups. Fecal pH in uninfected mice decreased slightly only in mice fed the 10% VF diet compared with the basal diet whereas no differences were seen among mice fed different VF diets in infected mice (ESI Fig. 1B†).

Excretion of *Cr* in the feces on days 4, 7, and 11 was used to monitor the infection. Previously we found that mice fed the basal TWD reduced colonization efficiency compared with mice fed the RPS diets and higher levels of colonization in mice fed the 10% RPS diet.[47] The reduced colonization efficiency was reproduced with 5 of 34 mice fed the TWD having an average 3 $\log_{10}$ lower *Cr* load than the average of the other TWD-fed infected mice, and these were excluded from the colonization analysis to ensure uniform infection kinetics. On day 4 post-infection, the remaining mice fed the TWD had a significantly lower *Cr* fecal load compared with infected mice fed the 5% and 10% VF diets (Fig. 2A). On days 7 and 11 post-infection only, the mice fed the 10% VF diet had a significantly higher *Cr* fecal load than mice fed the TWD (Fig. 2B and C). Mucosa depth was measured in hematoxylin and eosin-stained colon sections from a set of infected mice and increased with increasing dietary VF (Fig. 3A). Sections from infected mice were also scored for the degree of tissue pathology, and mice fed the 5% and 10% had greater pathology scores than did mice fed the TWD and 2% VF diet (Fig. 3B).

Effect of VF and *Cr* infection on the microbiome diversity and composition

Consumption of dietary fiber (DF) and RSs can alter the microbiome.[10,62] We previously showed that feeding raw potato starch[46] or VF[63] can alter the microbiome and that feeding RPS exacerbated *Cr*-induced colitis,[47] but the effects of VF, a phosphorylated, cross-linked potato starch, on the microbiome in *Cr* infected mice are unknown. To further investigate the effect of consuming VF on a subsequent *Cr* infection we looked for changes to the cecal microbiome, the primary site of fermentation in mice. In agreement with our previous findings, mice fed the 10% VF diet had decreased alpha-diversity as measured by the Shannon entropy diversity plots but not in the Chao 1 bias or Simpson plot (Fig. 4A–C). *Cr* infection did not further affect diversity. A Bray–Curtis beta-diversity plot of all 8 treatment groups showed substantial overlap among the uninfected and infected mice fed the basal TWD and 2% VF diets. In contrast, mice fed the 5% and especially the 10% VF diet were separated from the TWD/2% cluster with additional spatial separation of the uninfected and infected 5% and 10% VF groups from one another (Fig. 5). Bray–Curtis beta-diversity plots of only uninfected mice showed a clear separation of the 5% and 10% VF groups from the 0% and 2% VF groups (ESI Fig. 2A†) while infection resulted in a closer clustering of the 0, 2 and 5% VF groups with the 10% VF group still clearly separated from the rest (ESI Fig. 2B†).

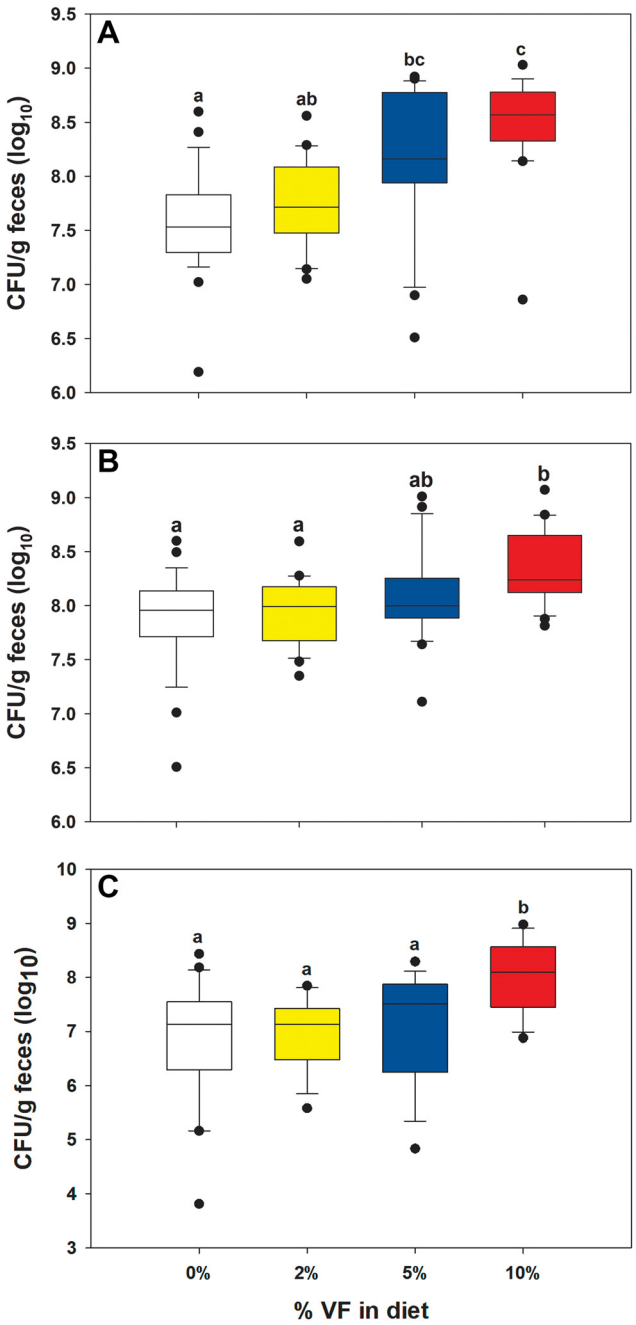

Fig. 2 Effect of VF consumption on fecal *Cr* excretion. *Cr* fecal excretion (CFU g^{-1} feces) was measured on (A) day 4, (B) day 7, and (C) day 11 PI in *Cr*-infected mice fed increasing levels of VF. Different letters indicate statistical significance at $p < 0.05$, $n = 15–29$ per group, pooled from three experiments.

As observed before,[63] uninfected mice fed VF had multiple dose-dependent changes to various genera with the greatest number of significant changes occurring in the 10% VF group. This was also true in *Cr*-infected VF-fed mice, and these changes are summarized in Fig. 6 and ESI Table 2.† Similar

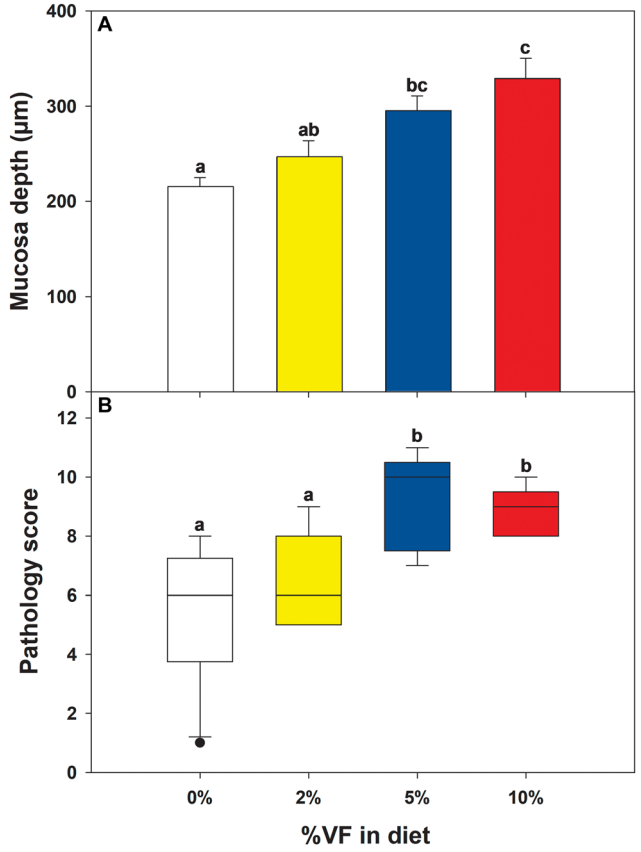

Fig. 3 Effect of VF consumption on mucosal depth and colon pathology in *Cr*-infected mice. (A) Mucosal depth and (B) pathology scores of distal colons from *Cr*-infected mice fed increasing levels of VF at day 12 post-infection. Groups with different letters indicate statistical significance at $p < 0.05$, $n = 5–10$ per group.

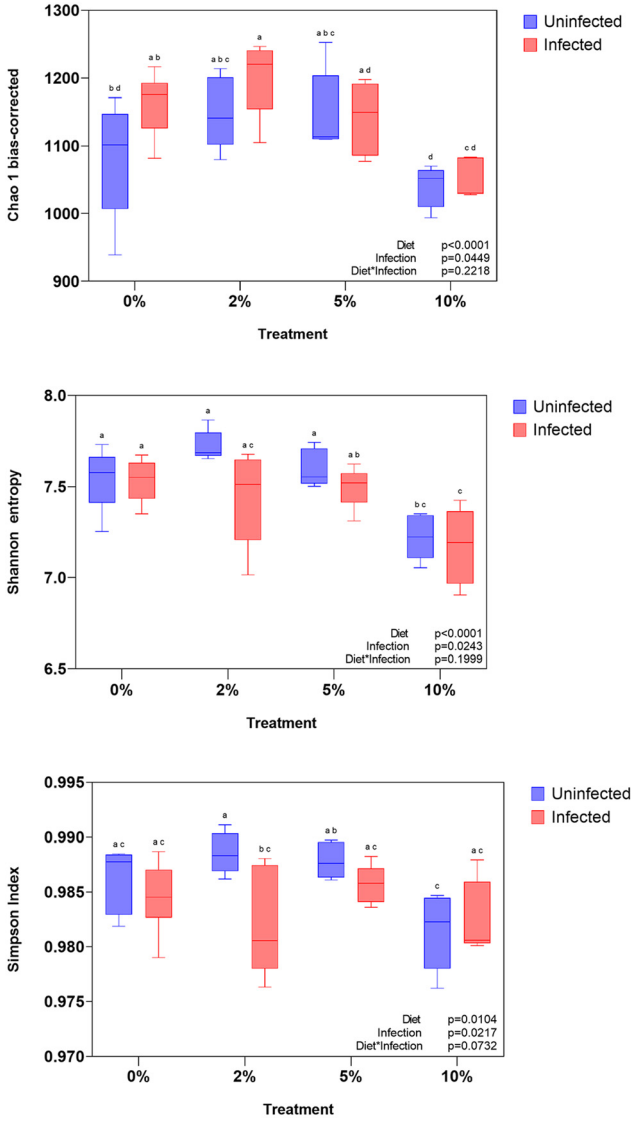

Fig. 4 Effect of VF consumption and *Cr* infection on cecal content alpha-diversity indices. Cecal contents were collected on day 12 post-infection in control and infected mice fed increasing levels of VF. (A) Chao-1 bias corrected (B) Shannon entropy (C) Simpson index. Different letters indicate statistical significance at $p < 0.05$, $n = 5–10$ per group.

numbers of genera had increased or decreased relative abundances (RAs) and many, but not all changes were of similar direction (up or down) in both infected and uninfected mice. This includes increases in *Bacteroides*, *Catenibacterium*, *Dubosiella*, *Lachnospiraceae NK4A136 group*, and *Muribaculum* and decreases in *Anaeroplasma*, *Bilophila*, *Clostridium sensu stricto 1*, *Rikenella*, *Roseburia*, and *Turicibacter* with increasing dietary VF. In some of these cases, however, the % relative abundance (RA) was significantly different between uninfected and infected genera (Fig. 6 and ESI Table 2†). Examples include increased RA of *Bifidobacterium*, *Catenibacterium*, *Clostridium sensu stricto 1*, *Desulfovibrio*, *Faecalibaculum*, *Lactobacillus*, *Ligilactobacillus*, and *Muribaculum* in infected compared with uninfected mice fed the basal diet, while the RA of *Bilophila* decreased in infected mice fed the basal diet. The RAs of *Rikenella* and *Turicibacter* were reduced in infected mice compared to uninfected mice irrespective of VF level. There were genera whose RA were uniquely increased or decreased in either uninfected or infected mice. In uninfected mice, *Bifidobacterium* and *Faecalibaculum* levels increased while *Lachnospiraceae GCA-900066575* decreased with increasing dietary VF while their RAs were not responsive to VF feeding in infected mice. *Blautia*, *Desulfovibrio*, *Lactobacillus*, *Ligilactobacillus* and *Staphylococcus* RAs did not change in uninfected mice but decreased in response to feeding VF in infected mice. Two genera, *Eisenbergiella* and *Limosilactobacillus* moved in opposite directions in uninfected *vs.* infected mice. The RA of an unknown genus in the family *Tannerellaceae* was markedly increased in infected mice fed the 10% VF diet. *Turicibacter* has been shown to be important for preventing severe disease in *Cr*-infected mice[64] and susceptibility to dextran sodium sulfate-induced colitis.[65] Its levels were higher in uninfected mice at all VF levels and was decreased significantly in mice fed the 10% VF diet in both uninfected and infected mice. While at day 12 post-infection the cecum is not a primary site of *Cr* replication, *Cr* was

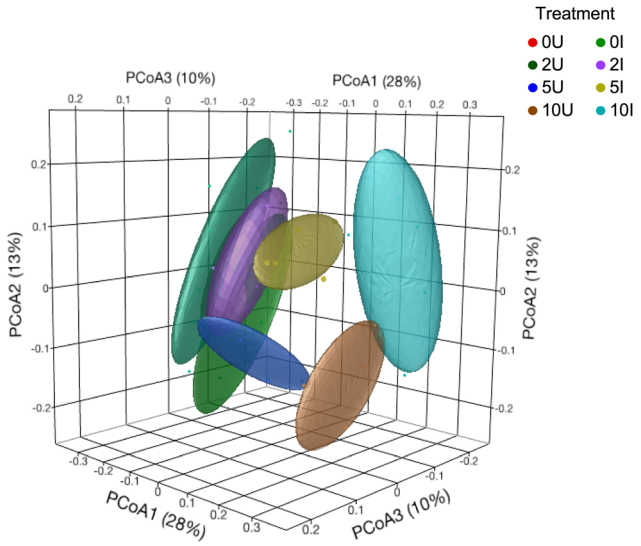

Fig. 5 Effect of VF consumption and *Cr* infection on cecal content beta-diversity. Bray-Curtis principal coordinates analysis (PCoA) plot showing greater beta diversity and separation of 5% and 10% VF-fed mice in both uninfected and *Cr*-infected mice (n = 5–10 per group).

detected in all infected groups and was significantly elevated in the 10% VF group compared with the other infected groups, mirroring what was observed with fecal *Cr* excretion at day 11 post-infection in mice fed the 10% VF diet.

Effect of VF and *Cr* infection on gene expression in the cecum and distal colon

We previously demonstrated that feeding VF had significant effects on gene expression in cecal and DC tissue that was most pronounced in mice fed the 10% VF diet, and the number of differentially expressed genes decreased from the cecum to the DC.[63] To explore potential mechanisms that could be associated with the increased *Cr* colonization and pathology in animals fed the 10% VF diet, we conducted RNASeq analysis on the cecum and DC of infected or control animals fed diets containing 0%, 2%, 5% or 10% VF. The eight groups of animals will be referred to in the text as follows: uninfected animals fed the control diet, 2%, 5%, or 10% VF will be referred to as 0U, 2U, 5U and 10U. Infected animals fed the control diet, 2%, 5% or 10% VF will be referred to as 0I, 2I, 5I and 10I. Comparisons will be referred to by an underscore (_). All pairwise comparisons for cecum and DC are found in ESI Tables 3 and 4,† respectively.

Because of space limitations, we will focus on three sets of comparisons when discussing genes and pathways unless otherwise indicated. In the first, the fold-change from the uninfected (2U_0U, 5U_0U or 10U_0U) comparisons will be compared to elucidate the magnitude of the changes due to differing levels of dietary VF in uninfected animals. In the second, changes in the 2I_0U, 5I_0U or 10I_0U comparisons will be compared with the changes in the 0I_0U comparison to elucidate the magnitude of changes due to diet and infection compared with those induced by *Cr* infection in the absence of dietary VF. In the third, changes in the 2I_0I, 5I_0I or 10I_0I comparisons will be compared with each other to elucidate how dietary VF is affecting gene expression due to infection.

Differentially expressed genes in cecum formed three distinct clusters by PCA (ESI Fig. 3A†) and two in DC (ESI Fig. 3B†). This is due to the overwhelming effect of infection. In the cecum, the comparisons with the greatest total number of DEGs were 10I_10U, 10I_5U, and 10I_0U and are summarized in ESI Table 5.† The ratio of down to upregulated genes in these comparisons was 1.2, 1.1 and 1.2, respectively. In the DC, the comparisons with the greatest total number of DEGs were 10I_0U, 5I_0U and 10I_2U (ESI Table 5†). The ratio of down to upregulated genes in these comparisons was 1.2, 1.3 and 1.2, respectively.

The number of cecal genes that were up- or downregulated ≥1.5 fold at an FDR adjusted p value <0.05 in 2U_0U, 5U_0U or 10U_0U comparisons is shown in ESI Table 5.† One, 35 and 195 genes were upregulated in the 2U_0U, 5U_0U, or 10U_0U comparisons, respectively. Three, 37 and 148 genes were downregulated by 2U_0U, 5U_0U or 10U_0U comparisons, respectively. A Venn analysis showed that of the 195 upregulated DEGs in the 10U_0U comparison, 166 were unique, and of the 148 down-regulated DEGs in the 10U_0U comparison, 115 were unique with few DEGs shared between comparisons (ESI Fig. 4A and B†). Only one upregulated gene, *Slc10a2*, encoding a sodium/bile acid cotransporter, was shared by all comparisons. Three genes were commonly downregulated in the cecum, *Zbed6*, *Cyp1a1* and *Cxcl10*.

The number of DC genes that were up- or downregulated ≥1.5-fold at an FDR-adjusted p value <0.05 in 2U_0U, 5U_0U or 10U_0U groups is shown in ESI Table 5.† In the DC, 4, 21, and 212 genes were upregulated by 2U_0U, 5U_0U, or 10U_0U, respectively. One, two and 134 genes were downregulated by 2U_0U, 5U_0U, or 10U_0U *versus* 0I_0U, respectively (ESI Table 5†). Venn analysis revealed ten upregulated genes exclusively in the 5U_0U comparison and 200 genes exclusively in the 10U_0U comparison (ESI Fig. 4C and D†). There were 132 downregulated genes exclusively in the 10U_0U comparison. Three upregulated genes, *Cd177*, *Duox2* and *Duoxa2*, were shared by all comparisons of VF upregulated genes. All of these genes are involved in the immune response. Only one gene, *Cyp1a1*, is commonly downregulated in the DC. In contrast to our previous study, where RPS downregulated a large number of genes involved in vitamin A (VA) metabolism, only one gene (*Cyp1a1*) was downregulated by all doses of VF in DC. Instead, several genes critical for active VA synthesis (*Rdh1* (10%), *Dhrs9* (5%, 10%) and *Rdh9* (10%)), were upregulated by VF alone in DC.

Thirteen goblet cell-associated genes, encompassing several broad categories, were significantly upregulated in uninfected animals by 10% VF alone, in DC; antibacterial/antiparasitic (*Ang4*,[66] 5.9-fold, $p = 3.87 \times 10^{-4}$, *Retnlb*,[67] 13.5-fold, $p = 2.92 \times 10^{-7}$, *Reg4*,[68] 2.2-fold, $p = 5.24 \times 10^{-3}$), chloride ion transport (*Slc9a3*,[69] 2.7-fold, $p = 3.84 \times 10^{-4}$, *Clca1*,[70] 1.6-fold, $p = 4.95 \times 10^{-2}$, *Clca4a*,[71] 2.9-fold, $p = 4.77 \times 10^{-3}$ and *Clca4b*,[71] 18.6-fold, $p = 1.43 \times 10^{-6}$), and mucin generation and secretion (*B3gnt2*

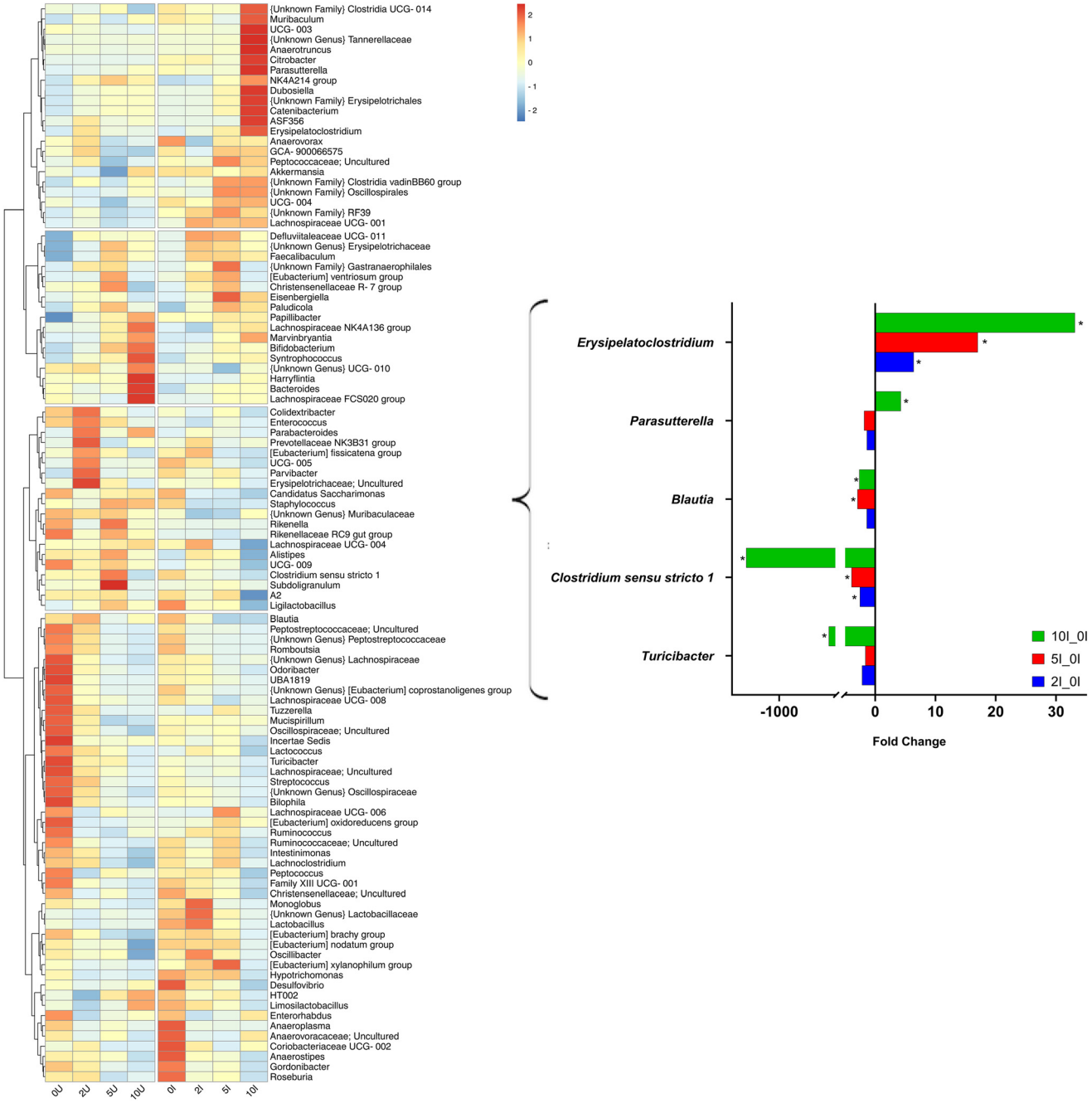

Fig. 6 Effect of VF consumption and *Cr* infection on the abundance of cecal bacterial genera. The differential abundance analysis was performed with the MaAslin2 and a relative abundance heatmap showing hierarchical clustering of normalized (*z*-score) bacterial genera abundances in cecal contents was generated using *pheatmap*. Intensity of color indicates the number of standard deviations above (red) and below (blue) the mean. Horizontal bar chart highlights fold changes in genera associated with altered susceptibility to *Cr*-infection found in *Cr*-infected mice (n = 5–10 per group).

1.7-fold,[72] $p = 5.16 \times 10^{-3}$, *Muc3a*[73] 1.5-fold, 3.21×10^{-2}, *Fut2*,[74] 1.5-fold $p = 4.58 \times 10^{-2}$, *St3gal1*,[75] 1.6-fold, $p = 4.82 \times 10^{-2}$, *St3gal3*,[76] 1.5-fold, $p = 4.21 \times 10^{-2}$, *Slc9a3*,[77] 2.7-fold, $p = 3.84 \times 10^{-4}$). Of note, more than half of these genes (*Ang4*,[78] *Clca1*,[70] *Clca4b*,[79] *Fut2*,[80] *Reg4*,[81] *Retnlb*,[82] and *Slc9a3*[83]) are upregulated by the Th2-assoiated cytokines, IL-4 and/or IL-13. With the exception of *Retnlb* and *St3gal1*, which were unchanged, and *Fut2*, which increased by 3-fold, the expression of these genes decreased after infection (10I_10U comparison), some such as *Ang4* (−6.0-fold), *Reg4* (−20.0-fold) and *Clca4b* (−64.0-fold) substantially so. This is not surprising as goblet cell depletion is a hallmark of *Cr* infections.[84,85]

In the cecum, a Venn analysis of genes that were up- or downregulated ≥1.5 fold, respectively, at an FDR-adjusted p

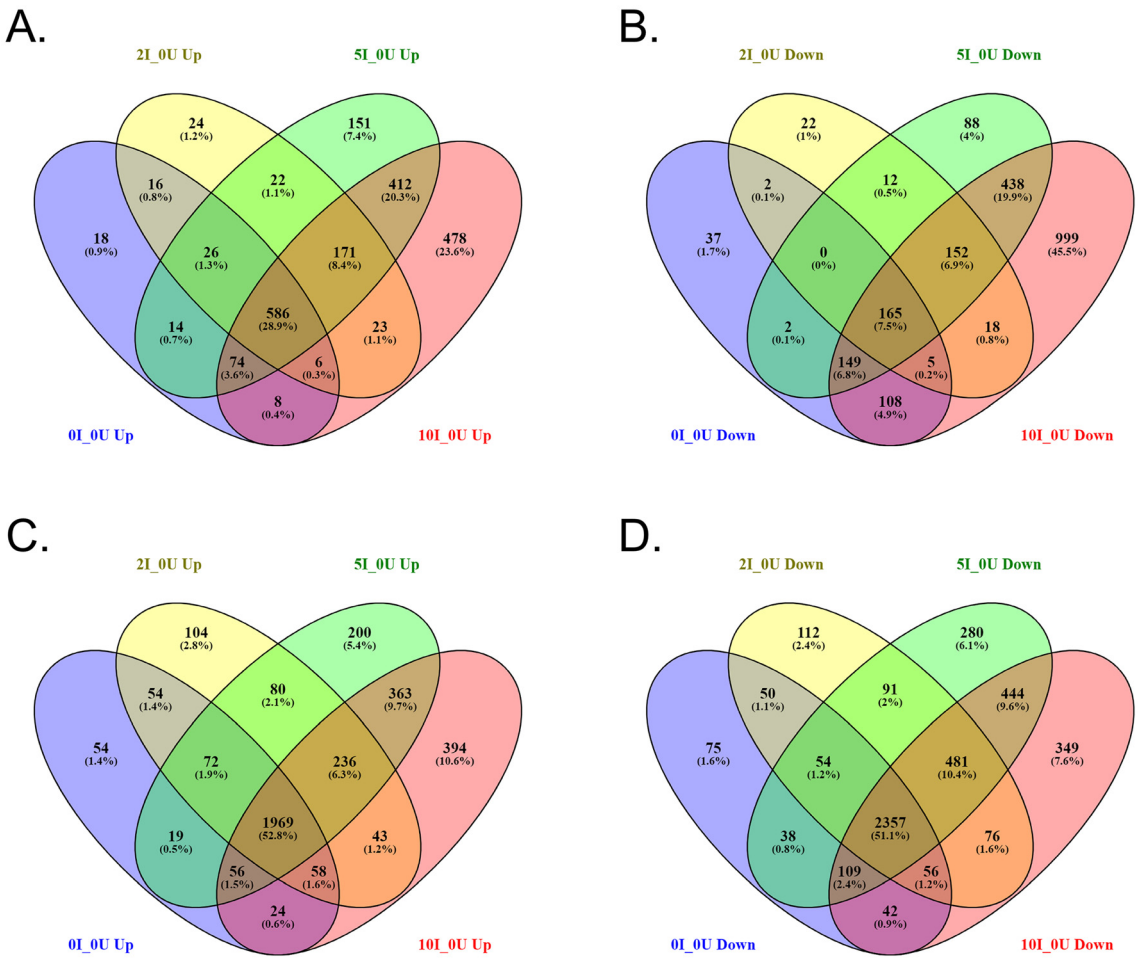

Fig. 7 Venn analysis of DEGs in the cecum and DC of *Cr*-infected mice fed different levels of VF compared with uninfected mice fed the basal diet. Venn analysis of upregulated (A, C) or downregulated (B, D) DEGs of *Cr*-infected mice fed different levels of VF compared with uninfected mice fed the basal diet (≥1.5-fold) in the cecum (A, B) and or DC (C, D). FDR adjusted $p < 0.05$, $n = 5$ per group.

value <0.05 in the 0I_0U, 2I_0U, 5I_0U or 10I_0U comparisons was performed to elucidate the magnitude of changes due to diet and infection compared with those induced by *Cr* infection in the absence of dietary VF and the results are shown in Fig. 7A and B. In the cecum, the number of genes that were commonly upregulated in 0I_0U, 2I_0U, 5I_0U and 10I_0U groups was 586, and 165 genes were commonly downregulated. A very large number of genes, 478 and 999 were exclusively up- or down-regulated in cecum in the 10I_0U group, respectively. In the DC, the number of genes that were commonly upregulated in the 0I_0U, 2I_0U, 5I_0U or 10I_0U groups was 1969 (Fig. 7C and D), while 2357 genes were commonly downregulated. As was seen in the cecum, in the DC many genes were exclusively up- (394) or down-regulated (349) in the 10I_0U group.

The top 20 up- or downregulated genes for comparisons 0I_0U, 2I_0U, 5I_0U and 10I_0U in the cecum and DC are shown in Tables 1 and 2, respectively. In the cecum, there were seven genes shared among the top 20 downregulated genes (*Iqcb1*, *Htr2b*, *Gm37019*, *Atp1a2*, *Ecscr*, *Gpr183* and *Cyp1a1*). Six upregulated genes were found in common among the comparisons (*Reg3b*, *Ly6f*, *Zfp968*, *Ighv1-54*, *Cxcr6* and *Ighv1-59*). *Reg3b* and *Ly6f* progressively increased in expression with increasing dietary VF concentrations. Three genes, *Nos2*, *Plet1* and *Utp14b*, were exclusively found in the top 20 genes of VF-treated comparisons (2I_0U, 5I_0U and 10I_0U) but not in the 0I_0U comparison.

In the DC, six genes, *Pln*, *Zbtb12*, *Iqcb1*, *Htr2b*, *Lrrc17* and *Angpt2*, were found in the top 20 list of all downregulated genes. The most highly downregulated gene in the DC was *Pln* (−2504.4, −2532.3, −2581.0, and −2549.2-fold in sequential order of VF supplementation) found in all infected *versus* uninfected comparisons. Similar to the cecum, there was a generalized increase in significance and fold change with increasing VF content of the diet. Fifteen upregulated genes were found in common in the top 20 for all groups, and of those, approximately $\frac{1}{2}$ of them can be classified into common functional groups: one REG Family Gene (*Reg3b*), three chemokines (*Cxcl3*, *Cxcl5*, *Cxcl11*), two calprotectins (*S100a8*, *S1009a*) and one LU Superfamily member (*Gml2*). The average expression

Table 1 Top 20 DEGs found in the cecum of *Cr*-infected mice[a]

Downregulated

0I_0U			2I_0U			5I_0U			10I_0U		
Gene[b]	FC	*p* (adj)	Gene	FC	*p* (adj)	Gene	FC	*p* (adj)	Gene	FC	*p* (adj)
Iqcb1	−406.8	3.64×10^{-4}	Tnfsf12	−156.6	3.04×10^{-2}	Iqcb1	−413.9	7.23×10^{-5}	Zbed6	−2058.2	1.04×10^{-5}
B3galt2	−240.2	9.64×10^{-3}	Htr2b	−155.8	1.45×10^{-2}	Cfap141	−309.5	6.50×10^{-4}	Pln	−966.2	1.84×10^{-5}
Htr2b	−157.2	1.57×10^{-2}	Atp1a2	−113.4	2.23×10^{-2}	Aldh4a1	−270.6	1.94×10^{-3}	Iqcb1	−403.7	1.15×10^{-4}
Gm37019	−119.4	2.03×10^{-2}	Ecscr	−109.9	1.56×10^{-2}	B3galt2	−244.7	3.57×10^{-3}	Depp1	−283.2	5.21×10^{-4}
Atp1a2	−114.4	2.38×10^{-2}	Sstr2	−99.9	2.01×10^{-2}	Tnfsf12	−160.9	1.50×10^{-2}	Aldh4a1	−263.8	2.07×10^{-3}
Ecscr	−110.8	1.69×10^{-2}	Gpr183	−90.0	3.04×10^{-2}	Htr2b	−160.0	6.23×10^{-3}	Cyp1a1	−238.3	4.11×10^{-15}
Aldh4a1	−94.5	2.04×10^{-3}	Ugt1a9	−76.7	4.40×10^{-2}	Cyp1a1	−157.1	1.76×10^{-13}	Gm38666	−221.2	1.24×10^{-4}
Gpr183	−90.8	3.21×10^{-2}	Cyp1a1	−65.6	2.56×10^{-9}	Gbp9	−124.9	1.69×10^{-4}	Htr2b	−156.0	6.14×10^{-3}
Ankrd23	−88.6	4.37×10^{-2}	Pcdhgb1	−54.9	4.16×10^{-3}	Gm37019	−121.5	8.27×10^{-3}	Gm37019	−118.5	8.17×10^{-3}
Xkrx	−84.4	3.33×10^{-2}	Zbed6	−54.3	1.37×10^{-4}	Atp1a2	−116.4	1.00×10^{-2}	Psapl1	−116.8	4.37×10^{-3}
Zbed6	−54.8	1.87×10^{-4}	Apoa4	−22.4	7.98×10^{-7}	Ecscr	−112.8	6.54×10^{-3}	Atp1a2	−113.5	9.75×10^{-3}
Psapl1	−45.4	2.80×10^{-3}	Cyp4a32	−21.9	8.10×10^{-10}	Sstr2	−102.6	8.66×10^{-3}	Ecscr	−110.0	6.71×10^{-3}
Gpr18	−28.2	3.29×10^{-2}	Iqcb1	−19.5	2.41×10^{-6}	Gpr183	−92.4	1.42×10^{-2}	Sstr2	−100.0	8.72×10^{-3}
Cyp1a1	−15.5	3.37×10^{-4}	Gm37019	−16.7	2.76×10^{-2}	Xkrx	−85.9	1.48×10^{-2}	Gpr183	−90.1	1.37×10^{-2}
Slc35g3	−11.8	3.44×10^{-2}	Gm49373	−15.1	5.39×10^{-3}	Gm48552	−74.6	2.60×10^{-2}	Ankrd23	−88.0	1.94×10^{-2}
Irs4	−9.0	4.74×10^{-2}	Gm49366	−14.8	6.63×10^{-3}	Cyp2c69	−64.8	9.77×10^{-3}	Xkrx	−83.8	1.44×10^{-2}
G0s2	−8.1	1.68×10^{-2}	1700057G04Rik	−14.2	6.89×10^{-10}	Pcdhgb6	−56.6	3.15×10^{-2}	Ugt1a9	−76.8	2.05×10^{-2}
Apoa4	−7.1	8.53×10^{-4}	Ugt8a	−13.2	4.01×10^{-12}	Alas2	−51.0	3.85×10^{-2}	1700057G04Rik	−68.8	4.87×10^{-12}
Ajap1	−7.0	2.39×10^{-2}	Cyp4b1	−11.8	1.53×10^{-23}	St6galnac2_2	−47.0	4.31×10^{-2}	Trpv6	−67.1	1.13×10^{-16}
Pln	−6.6	2.71×10^{-2}	Cyp2c69	−10.5	7.19×10^{-3}	Rsph14	−46.1	4.28×10^{-2}	H2bc23	−63.3	4.08×10^{-2}

Upregulated

0I_0U			2I_0U			5I_0U			10I_0U		
Gene	FC	*p* (adj)	Gene	FC	*p* (adj)	Gene	FC	*p* (adj)	Gene	FC	*p* (adj)
Ighv1-75	62.0	5.32×10^{-13}	Nos2	71.0	7.67×10^{-36}	Utp14b	88.0	2.21×10^{-2}	Fpr2	108.4	5.55×10^{-3}
Reg3b	71.5	1.14×10^{-11}	Skint8	76.5	1.92×10^{-2}	Ighv1-61	89.4	7.53×10^{-3}	Cxcl5	110.1	1.78×10^{-10}
Igkv13-85	72.5	8.39×10^{-16}	Ighv1-61	78.0	1.62×10^{-2}	Mtcp1	92.2	1.57×10^{-2}	Ighv10-3	112.9	3.71×10^{-3}
Ighv3-4	73.0	4.69×10^{-2}	Igkv1-88	79.1	2.94×10^{-2}	Phyhd1	96.2	1.87×10^{-2}	Ighv1-54	117.8	8.26×10^{-17}
Igkv6-13	79.6	3.40×10^{-5}	Atp12a	81.0	1.65×10^{-2}	Ighv13-2	99.0	4.18×10^{-5}	Ighv2-6	122.2	6.29×10^{-3}
Gm9860	84.4	2.93×10^{-2}	Ighv1-75	81.6	4.60×10^{-15}	Ighv3-4	99.9	1.63×10^{-2}	Plet1	144.8	1.21×10^{-44}
Ighv8-5	90.4	2.46×10^{-2}	Ighv1-63	89.9	2.74×10^{-11}	Pla2g2a	100.2	1.74×10^{-7}	2310034C09Rik	152.1	1.19×10^{-3}
Ighv1-61	96.4	1.23×10^{-2}	Igkv14-130	98.2	2.27×10^{-2}	Reg3g	101.5	3.92×10^{-23}	Pla2g2a	154.7	4.42×10^{-9}
Igkv1-88	96.6	2.38×10^{-2}	Ighv1-43	102.1	2.00×10^{-2}	Ighv2-6	113.8	1.10×10^{-2}	Reg3g	171.9	6.09×10^{-29}
Igkv4-53	100.1	8.63×10^{-22}	Gm43720	103.7	3.92×10^{-2}	Plet1	133.2	6.14×10^{-43}	Nos2	254.4	5.92×10^{-61}
Ly6f	104.5	6.42×10^{-3}	Zfp968	105.6	1.19×10^{-3}	Gm9860	141.0	6.01×10^{-3}	Zfp968	257.5	1.78×10^{-5}
Ighv2-6	105.0	2.35×10^{-2}	Plet1	114.7	7.49×10^{-40}	Ighv1-63	146.6	2.44×10^{-14}	Clca4b	258.2	6.25×10^{-44}
Ighv10-3	108.9	1.19×10^{-2}	Ly6f	149.3	2.06×10^{-3}	Clca4b	177.0	6.33×10^{-38}	Utp14b	292.6	1.40×10^{-3}
Ighv1-74	123.0	3.96×10^{-16}	Ighv1-54	157.3	4.20×10^{-18}	Nos2	180.1	2.81×10^{-53}	Tmem253	339.6	7.40×10^{-4}
Atp12a	156.7	4.91×10^{-3}	Utp14b	158.6	1.24×10^{-2}	Ighv1-54	206.3	1.34×10^{-20}	Gm28040_2	388.6	4.80×10^{-4}
Zfp968	167.5	3.64×10^{-4}	Reg3b	162.6	6.63×10^{-17}	Zfp968	216.7	5.53×10^{-5}	Reg3b	433.4	9.11×10^{-25}
Ighv1-54	173.7	1.28×10^{-18}	Phyhd1	184.5	9.21×10^{-3}	Reg3b	261.1	1.32×10^{-20}	Ly6f	482.5	1.98×10^{-5}
Ighv1-63	204.5	1.49×10^{-15}	Ighv3-4	330.6	2.42×10^{-3}	Ly6f	459.8	3.78×10^{-5}	Gm9860	569.3	1.27×10^{-4}
Cxcr6	316.9	4.87×10^{-4}	Ighv1-59	393.9	2.78×10^{-14}	Ighv1-59	1136.2	3.21×10^{-20}	Ighv1-59	962.1	1.49×10^{-19}
Ighv1-59	436.0	1.55×10^{-14}	Cxcr6	507.0	8.32×10^{-5}	Cxcr6	1498.3	8.86×10^{-7}	Cxcr6	1140.8	1.59×10^{-6}

[a] Genes that were up- or downregulated ≥1.5 fold were considered significant at an FDR-adjusted $p < 0.05$, $n = 5$. [b] Genes shared between comparisons.

Table 2 Top 20 DEGs found in the distal colon of *Cr*-infected mice[a]

Downregulated

0I_0U			2I_0U			5I_0U			10I_0U		
Gene[b]	FC	*p* (adj)	Gene	FC	*p* (adj)	Gene	FC	*p* (adj)	Gene	FC	*p* (adj)
Pln	−2504.4	2.29×10^{-6}	Pln	−2532.3	1.98×10^{-8}	Pln	−2581.0	1.67×10^{-8}	Pln	−2549.2	1.23×10^{-8}
Zbtb12	−869.3	3.11×10^{-6}	Slc39a5	−939.5	7.31×10^{-6}	Sycp3	−1011.5	8.41×10^{-6}	Sycp3	−999.0	7.04×10^{-6}
Iqcb1	−428.6	8.95×10^{-5}	B3galt2	−915.7	5.29×10^{-5}	Slc39a5	−957.7	6.20×10^{-6}	Slc39a5	−945.8	5.15×10^{-6}
Tmem204	−400.0	4.09×10^{-4}	Zbtb12	−876.1	3.16×10^{-5}	B3galt2	−933.5	4.45×10^{-5}	B3galt2	−921.9	3.85×10^{-5}
Yod1	−302.1	1.44×10^{-3}	Gbp9	−752.3	2.57×10^{-5}	Zbtb12	−888.7	1.57×10^{-6}	Zbtb12	−877.7	1.25×10^{-6}
Htr2b	−247.1	1.91×10^{-3}	Afmid	−600.4	9.79×10^{-5}	Cyp1a1	−662.3	8.32×10^{-9}	Cyp1a1	−664.9	7.52×10^{-9}
Lrrc17	−240.8	1.08×10^{-3}	Nnat	−533.0	5.05×10^{-4}	Nnat	−543.3	4.28×10^{-4}	Nnat	−536.6	3.92×10^{-4}
Angpt2	−158.2	4.10×10^{-3}	Cfap141	−513.9	7.46×10^{-5}	Cfap141	−523.9	6.36×10^{-5}	Sstr2	−464.2	1.59×10^{-5}
Gm37019	−118.6	7.21×10^{-3}	Sstr2	−461.2	2.23×10^{-5}	Sstr2	−470.0	1.92×10^{-5}	Iqcb1	−432.8	4.39×10^{-5}
Atp1a2	−93.7	1.47×10^{-2}	Iqcb1	−429.9	6.03×10^{-5}	Iqcb1	−438.2	5.18×10^{-5}	Cyp2c55	−321.6	1.74×10^{-23}
Ecscr	−91.1	1.30×10^{-2}	Methig1	−377.4	2.64×10^{-9}	Gpr22	−402.2	3.99×10^{-5}	Htr2b	−249.6	1.16×10^{-3}
Xirp1	−75.9	7.02×10^{-3}	Cyp1a1	−303.8	1.59×10^{-9}	Pla2g4b	−377.7	2.31×10^{-4}	Lrrc17	−243.1	6.22×10^{-4}
Ankrd23	−66.9	3.26×10^{-2}	Yod1	−303.1	1.10×10^{-3}	Cyp2c55	−368.3	3.35×10^{-24}	Mettl7a2	−194.7	5.14×10^{-18}
Aldh4a1	−66.8	1.89×10^{-2}	Htr2b	−247.9	1.46×10^{-3}	Slc30a10	−310.3	6.27×10^{-24}	Slc30a10	−193.8	4.68×10^{-24}
Cox8b	−61.4	1.02×10^{-2}	Lrrc17	−241.5	7.98×10^{-4}	Htr2b	−252.7	1.26×10^{-3}	Cyp2c69	−179.8	9.45×10^{-9}
Lhpp	−48.4	2.91×10^{-2}	Mettl7a2	−235.9	2.12×10^{-17}	Lrrc17	−246.2	6.87×10^{-4}	Grin2b	−167.8	5.39×10^{-4}
6330411D24Rik	−44.1	1.78×10^{-2}	Gm21083	−219.4	3.08×10^{-4}	Gm21083	−223.6	2.67×10^{-4}	Angpt2	−159.7	2.59×10^{-3}
H2bc26-ps	−41.5	3.08×10^{-2}	Angpt2	−158.7	3.19×10^{-3}	Angpt2	−161.7	2.78×10^{-3}	Gm37019	−119.8	4.73×10^{-3}
G6pc2	−39.6	9.86×10^{-4}	Gm43720	−127.7	1.44×10^{-2}	Yod1	−108.9	2.79×10^{-4}	G6pc2	−104.4	2.79×10^{-3}
Ucn3	−36.7	3.33×10^{-2}	Gm37019	−119.0	5.76×10^{-3}	Atp1a2	−95.8	1.08×10^{-2}	Odf3b	−101.2	3.72×10^{-14}

Upregulated

0I_0U			2I_0U			5I_0U			10I_0U		
Gene	FC	*p* (adj)	Gene	FC	*p* (adj)	Gene	FC	*p* (adj)	Gene	FC	*p* (adj)
Myot	219.0	2.16×10^{-4}	Trim10	233.1	1.11×10^{-9}	Myot	345.6	3.30×10^{-5}	Cyp2j11	493.0	1.44×10^{-5}
Ltf	238.4	2.31×10^{-8}	Cyp2j11	238.3	1.90×10^{-4}	Trim10	348.9	3.30×10^{-11}	Nos2	558.2	1.29×10^{-84}
Reg3a	298.9	5.85×10^{-4}	Sprr2k	248.1	1.66×10^{-4}	Ltf	375.4	5.17×10^{-10}	Sprr2f	619.1	4.36×10^{-5}
Fpr2	302.6	2.24×10^{-4}	Prss22	311.7	6.98×10^{-5}	Nos2	497.6	1.76×10^{-81}	Gml2	825.5	1.77×10^{-6}
Sprr2k	321.1	9.59×10^{-5}	Cxcl11	321.7	6.90×10^{-5}	Pcdhgb2	513.4	2.28×10^{-4}	Il36g	854.4	1.87×10^{-6}
Cxcl11	335.2	7.72×10^{-5}	Fpr2	327.3	1.45×10^{-4}	Cxcl3	539.6	8.07×10^{-6}	Cxcl3	892.2	1.19×10^{-6}
Nos2	337.8	2.47×10^{-71}	Nos2	367.3	1.76×10^{-73}	Prss22	577.8	7.03×10^{-6}	Sprr2h	917.0	8.69×10^{-45}
Ifng	350.7	4.94×10^{-5}	Ifng	405.0	2.36×10^{-5}	Cxcl11	714.1	3.68×10^{-6}	Fpr2	932.7	3.96×10^{-6}
Reg2	356.5	3.62×10^{-7}	Reg3a	408.8	2.12×10^{-4}	Gm9860	809.0	5.28×10^{-6}	Ltf	1030.5	2.30×10^{-13}
Cxcl3	358.8	5.24×10^{-5}	Cxcl3	519.2	1.17×10^{-5}	Sprr2h	844.0	9.59×10^{-44}	Gm9860	1037.6	2.06×10^{-6}
Il36g	453.7	3.02×10^{-5}	Sprr2h	525.9	1.38×10^{-37}	Ifng	889.9	1.07×10^{-6}	Ifng	1064.2	4.95×10^{-7}
Sprr2h	489.1	1.40×10^{-36}	Il36g	544.8	1.26×10^{-5}	Gml2	909.5	1.31×10^{-6}	Cxcl11	1084.3	7.20×10^{-7}
Cxcl5	491.5	3.06×10^{-55}	Cxcl5	640.6	3.05×10^{-60}	Fpr2	952.2	3.92×10^{-6}	Prss22	1102.1	5.92×10^{-7}
Gml2	789.3	3.85×10^{-6}	Gm9860	822.8	6.33×10^{-6}	Cxcl5	1000.7	8.29×10^{-69}	Cxcl5	1155.1	8.69×10^{-72}
Gm9860	838.9	7.86×10^{-6}	Gml2	862.0	2.07×10^{-6}	Il36g	1089.8	7.92×10^{-7}	Clca4b	1189.5	1.03×10^{-47}
S100a9	888.1	7.35×10^{-13}	Clca4b	1113.3	2.44×10^{-46}	Clca4b	1269.8	1.34×10^{-48}	Sprr2d	1936.7	4.90×10^{-7}
Clca4b	900.0	1.42×10^{-43}	S100a9	1258.2	2.51×10^{-14}	S100a9	2584.3	1.90×10^{-17}	S100a8	2279.4	1.02×10^{-16}
S100a8	1044.0	2.77×10^{-13}	S100a8	1309.5	2.64×10^{-14}	S100a8	2625.2	2.67×10^{-17}	S100a9	3281.2	1.86×10^{-18}
Reg3b	1643.7	2.10×10^{-7}	Reg3b	3077.0	1.01×10^{-8}	Reg3b	3528.2	3.87×10^{-9}	Cxcr6	3359.0	1.85×10^{-9}
Cxcr6	2770.2	1.03×10^{-8}	Cxcr6	4138.9	1.03×10^{-9}	Cxcr6	4670.4	3.93×10^{-10}	Reg3b	5842.2	3.42×10^{-10}

[a] Genes that were up- or downregulated ≥1.5 fold were considered significant at an FDR-adjusted $p < 0.05$, $n = 5$. [b] Genes shared between comparisons.

levels of the genes exhibited a general dose-dependent pattern with the highest induction in the 10I_0U comparison followed by the 5I_0U, 2I_0U and then 0I_0U level. In DC, *Reg3b* was one of the most highly expressed gene in all groups and its expression increased in a dose-dependent manner (1643.7, 3077, 3528.2 and 5842.2-fold) in 0I_0U, 2I_0U, 5I_0U and 10I_0U comparisons, respectively. Several other gene pathways were parsed out for further analysis. Tables 3 and 4 contain data for selected cytokines and markers of inflammation in the cecum and DC, respectively.

All pairwise comparisons were analyzed for pathway enrichment using the online tool DAVID and embedded Reactome databases. Unique and shared pathways were identified by Venn analysis (Fig. 8). ESI Tables 6 and 7† contain the summary of all identified 0I_0U, 2I_0U, 5I_0U and 10I_0U Reactome pathways for the cecum and DC, respectively. ESI Table 8† contains a summary of I_0U pathway changes. ESI Table 9† contains data on DC cell cycle pathways and individual DC cell cycle genes.

The DAVID Analysis of Reactome pathways for DC revealed a dose-dependent increase in the number of genes

Table 3 Selected up- and down-regulated genes in the cecum of *Cr*-infected mice

		A		B		C		D		K		L		M	
Statistical code		0I_0U		2I_0U		5I_0U		10I_0U		2I_0I		5I_0I		10I_0I	
Categorization	Gene	FC	*p* (adj)	FC	*p* (adj)	FC	*p* (adj)	FC	*p* (adj)	FC	*p* (adj)	FC	*p* (adj)	FC	*p* (adj)
Th1-associated	Ifng	4.6	NS	5.9	2.32×10^{-2}	10.8	3.55×10^{-4}	15.8	1.21×10^{-5}	1.3	NS	2.3	NS	3.4	NS
	Socs1	2.9	4.59×10^{-4}	2.4	4.00×10^{-3}	4.3	6.42×10^{-8}	6.6	3.52×10^{-13}	−1.2	NS	1.5	NS	2.3	1.03×10^{-2}
	Socs3	4.0	2.19×10^{-10}	6.4	7.45×10^{-19}	8.8	1.26×10^{-26}	13.9	3.99×10^{-39}	1.6	NS	2.2	3.84×10^{-3}	3.5	2.85×10^{-8}
	Ido1	3.6	2.74×10^{-7}	2.4	8.18×10^{-4}	5.3	6.74×10^{-13}	7.6	2.46×10^{-19}	−1.5	NS	1.5	NS	2.1	7.84×10^{-3}
	Nos2	54.6	8.28×10^{-31}	71.0	7.67×10^{-36}	180.1	2.81×10^{-53}	254.4	5.92×10^{-61}	1.3	NS	3.3	3.02×10^{-3}	4.7	7.13×10^{-6}
TH17-associated	Il17a	2.7	NS	40.8	NS	20.8	NS	46.6	2.02×10^{-2}	15.1	NS	7.7	NA	17.3	3.80×10^{-2}
	Il17c	1.8	NS	1.9	NS	1.9	NS	2.5	NS	1.1	NS	1.1	NA	1.4	NS
	Il22	1.1	NS	−1.1	NS	−1.4	NS	3.3	NS	−1.2	NS	−1.6	NA	3.1	NS
	Il22ra2	−1.6	NS	−2.2	NS	−5.2	2.27×10^{-6}	−14.2	6.43×10^{-14}	−1.4	NS	−3.3	8.90×10^{-3}	−9.0	1.64×10^{-8}
Il1 superfamily and receptors	Il1b	3.2	1.09×10^{-3}	4.2	1.46×10^{-5}	6.3	2.30×10^{-9}	10.4	4.58×10^{-15}	1.3	NS	2.0	NS	3.2	5.17×10^{-4}
	Il33	1.2	NS	1.7	NS	2.1	NS	2.1	4.11×10^{-2}	1.4	NS	1.7	NS	1.7	NS
	Il1r2	1.2	NS	1.0	NS	2.1	NS	2.1	NS	−1.2	NS	1.7	NS	1.7	NS
	Il36a	−2.6	NA	3.6	NA	3.8	NS	−2.6	NS	9.3	NS	10.0	NS	1.0	NA
	Il36g	7.5	NS	15.1	NS	25.7	NS	20.3	NS	2.0	NS	3.4	NA	2.7	NS
Inflammation biomarkers	Lcn2	1.7	NS	2.5	NS	3.0	1.61×10^{-2}	3.3	5.51×10^{-3}	1.5	NS	1.8	NS	2.0	NS
	Il6	1.2	NS	2.1	NS	4.3	NS	4.0	NS	1.7	NS	3.5	NS	3.2	NS
	S100a9	5.7	NS	3.0	NS	9.6	9.06×10^{-3}	12.9	1.52×10^{-3}	−1.9	NS	1.7	NS	2.2	NS
	S100a8	8.1	NS	9.7	NS	7.0	NS	29.1	NS	1.2	NS	−1.2	NS	3.6	NS
	Tnf	4.7	1.19×10^{-8}	5.7	2.60×10^{-11}	10.4	4.57×10^{-21}	13.8	1.17×10^{-26}	1.2	NS	2.2	1.48×10^{-2}	3.0	7.05×10^{-5}
CXCL chemokines	Cxcl1	6.8	2.92×10^{-3}	10.2	9.56×10^{-5}	16.6	3.27×10^{-7}	26.2	8.89×10^{-10}	1.5	NS	2.4	NS	3.8	1.66×10^{-2}
	Cxcl2	12.0	1.15×10^{-2}	22.9	4.26×10^{-4}	35.7	1.47×10^{-5}	54.3	5.25×10^{-7}	1.9	NS	3.0	NS	4.5	3.76×10^{-2}
	Cxcl3	9.8	NS	18.6	NS	47.6	3.80×10^{-2}	63.7	1.60×10^{-2}	1.9	NS	4.8	NS	6.5	NS
	Cxcl5	20.9	3.84×10^{-4}	45.9	1.25×10^{-6}	82.4	4.17×10^{-9}	110.1	1.78×10^{-10}	2.2	NS	3.9	NS	5.3	6.47×10^{-3}
	Cxcl9	8.3	1.10×10^{-11}	8.2	8.19×10^{-12}	20.6	9.23×10^{-25}	25.6	9.97×10^{-29}	−1.0	NS	2.5	2.89×10^{-2}	3.1	1.13×10^{-3}
	Cxcl10	8.1	2.52×10^{-6}	7.3	6.77×10^{-6}	19.4	2.56×10^{-13}	26.6	2.05×10^{-16}	−1.1	NS	2.4	NS	3.3	1.66×10^{-2}
	Cxcl11	1.0	NS	1.0	NS	−1.0	NS	55.9	2.02×10^{-2}	1.0	NS	−1.0	NS	55.5	NA
	Ppbp	−6.6	NS	−2.2	NS	−27.7	NS	−1.7	NS	3.0	NS	−4.2	NS	3.9	NS
Goblet cell markers	Reg3b	71.5	1.14×10^{-11}	162.6	6.63×10^{-17}	261.1	1.32×10^{-20}	433.4	9.11×10^{-25}	2.3	NS	3.7	NS	6.1	9.78×10^{-3}
	Reg3g	29.9	4.44×10^{-12}	65.4	1.63×10^{-18}	101.5	3.92×10^{-23}	171.9	6.09×10^{-29}	2.2	NS	3.4	NS	5.8	1.09×10^{-3}
	Reg4	−1.4	1.92×10^{-2}	−1.6	2.91×10^{-5}	−2.3	1.05×10^{-14}	−2.5	5.66×10^{-19}	−1.2	NS	−1.7	1.45×10^{-4}	−1.8	1.47×10^{-7}

Table 4 Selected up- and down-regulated genes in the distal colon of *Cr*-infected mice

		A		B		C		D		K		L		M	
Statistical code		0I_0U		2I_0U		5I_0U		10I_0U		2I_0I		5I_0I		10I_0I	
Categorization	Gene	FC	*p* (adj)	FC	*p* (adj)	FC	*p* (adj)	FC	*p* (adj)	FC	*p* (adj)	FC	*p* (adj)	FC	*p* (adj)
Th1-associated	Ifng	350.7	4.94×10^{-5}	405.0	2.36×10^{-5}	889.9	1.07×10^{-6}	1064.2	4.95×10^{-7}	1.2	NS	2.5	4.93×10^{-2}	3.0	1.43×10^{-2}
	Socs1	12.9	1.69×10^{-25}	14.5	5.80×10^{-28}	18.1	5.07×10^{-33}	28.2	9.78×10^{-44}	1.1	NS	1.4	NS	2.2	2.00×10^{-2}
	Socs3	8.9	9.53×10^{-17}	13.7	5.28×10^{-24}	16.7	7.29×10^{-28}	19.2	1.26×10^{-30}	1.5	NS	1.9	NS	2.2	3.93×10^{-2}
	Ido1	134.4	8.03×10^{-50}	106.4	2.49×10^{-45}	138.2	4.97×10^{-54}	319.6	1.28×10^{-69}	−1.3	NS	1.0	NS	2.4	NS
	Nos2	337.8	2.47×10^{-71}	367.3	1.76×10^{-73}	497.6	8.65×10^{-86}	558.2	1.29×10^{-84}	1.1	NS	1.5	NS	1.7	NS
TH17-associated	Il17a	14.3	1.56×10^{-4}	20.2	1.09×10^{-5}	36.6	5.68×10^{-8}	30.3	2.92×10^{-7}	1.4	NS	2.5	NS	2.1	NS
	Il17c	2.3	NS	6.3	9.46×10^{-4}	5.1	3.42×10^{-3}	5.0	4.00×10^{-3}	2.7	NS	2.2	NS	2.1	NS
	Il22	16.1	3.63×10^{-3}	32.7	1.21×10^{-4}	62.7	2.66×10^{-6}	53.6	6.28×10^{-6}	2.0	NS	3.9	NS	3.3	NS
	Il22ra2	−2.4	4.01×10^{-4}	−2.5	1.52×10^{-4}	−2.8	1.05×10^{-5}	−6.0	3.10×10^{-14}	−1.0	NS	−1.2	NS	−2.5	4.45×10^{-3}
Il1 superfamily and receptors	Il1b	9.4	5.48×10^{-18}	17.3	3.83×10^{-29}	33.3	2.82×10^{-44}	28.1	3.91×10^{-40}	1.8	NS	3.5	2.29×10^{-5}	3.0	4.45×10^{-4}
	Il33	1.4	NS	1.9	3.77×10^{-3}	3.4	9.11×10^{-9}	3.6	1.90×10^{-9}	1.4	NS	2.5	1.25×10^{-3}	2.6	4.33×10^{-4}
	Il1r2	4.8	5.46×10^{-7}	6.0	4.03×10^{-9}	11.9	3.80×10^{-17}	10.3	3.17×10^{-15}	1.2	NS	2.5	1.16×10^{-2}	2.1	4.30×10^{-2}
	Il36a	22.7	NS	38.2	2.46×10^{-2}	44.5	1.66×10^{-2}	33.2	2.85×10^{-2}	1.7	NS	2.0	NA	1.5	NS
	Il36g	453.7	3.02×10^{-5}	544.8	1.26×10^{-5}	1089.8	7.92×10^{-7}	854.4	1.87×10^{-6}	1.2	NS	2.4	NS	1.9	NS
Inflammation biomarkers	Lcn2	9.1	5.24×10^{-12}	8.7	9.76×10^{-12}	21.3	3.50×10^{-23}	20.7	9.67×10^{-23}	−1.0	NS	2.3	3.25×10^{-2}	2.3	4.18×10^{-2}
	Il6	5.6	NS	15.8	4.78×10^{-4}	30.7	6.63×10^{-6}	22.6	4.52×10^{-5}	2.8	NS	5.5	3.35×10^{-2}	4.0	NS
	S100a9	888.1	7.35×10^{-13}	1258.2	2.51×10^{-14}	2584.3	1.90×10^{-17}	3281.2	1.86×10^{-18}	1.4	NS	2.9	NS	3.7	3.62×10^{-2}
	S100a8	1044.0	2.77×10^{-13}	1309.5	2.64×10^{-14}	2625.2	2.67×10^{-17}	2279.4	1.02×10^{-16}	1.3	NS	2.5	NS	2.2	NS
	Tnf	23.4	6.95×10^{-35}	27.8	7.16×10^{-39}	31.5	3.31×10^{-42}	38.0	7.91×10^{-47}	1.2	NS	1.3	NS	1.6	NS
CXCL chemokines	Cxcl1	14.5	1.11×10^{-13}	19.0	1.08×10^{-16}	28.0	1.77×10^{-21}	30.3	1.83×10^{-22}	1.3	NS	1.9	NS	2.1	NS
	Cxcl2	94.5	1.31×10^{-20}	102.2	1.57×10^{-21}	179.1	3.24×10^{-27}	214.8	3.92×10^{-29}	1.1	NS	1.9	NS	2.3	NS
	Cxcl3	358.8	5.24×10^{-5}	519.2	1.17×10^{-5}	539.6	8.07×10^{-6}	892.2	1.19×10^{-6}	1.4	NS	1.5	NS	2.5	NS
	Cxcl5	491.5	3.06×10^{-55}	640.6	3.05×10^{-60}	1000.7	8.29×10^{-69}	1155.1	8.69×10^{-72}	1.3	NS	2.0	NS	2.3	NS
	Cxcl9	41.5	2.61×10^{-40}	48.8	4.9×10^{-44}	71.2	4.53×10^{-53}	77.6	1.96×10^{-55}	1.2	NS	1.7	NS	1.9	NS
	Cxcl10	13.7	1.52×10^{-16}	15.7	2.00×10^{-18}	27.1	2.07×10^{-26}	30.5	2.46×10^{-28}	1.1	NS	2.0	NS	2.2	NS
	Cxcl11	335.2	7.72×10^{-5}	321.7	6.90×10^{-5}	714.1	3.68×10^{-6}	1084.3	7.20×10^{-7}	−1.0	NS	2.1	NS	3.2	4.71×10^{-2}
	Ppbp	1.3	NS	1.6	NS	2.5	NS	78.3	1.60×10^{-6}	1.2	NS	1.9	NS	59.3	3.64×10^{-4}
Goblet cell markers	Reg3b	1643.7	2.10×10^{-7}	3077.0	1.01×10^{-8}	3528.2	3.87×10^{-9}	5842.2	3.42×10^{-10}	1.9	NS	2.1	NS	3.6	9.71×10^{-3}
	Reg3g	34.3	1.73×10^{-19}	60.6	2.56×10^{-26}	76.0	1.61×10^{-29}	118.3	9.77×10^{-36}	1.8	NS	2.2	NS	3.4	9.11×10^{-3}
	Reg4	−4.7	6.19×10^{-14}	−6.8	6.00×10^{-21}	−7.1	3.17×10^{-22}	−9.2	6.21×10^{-28}	−1.4	NS	−1.5	NS	−1.9	2.25×10^{-2}

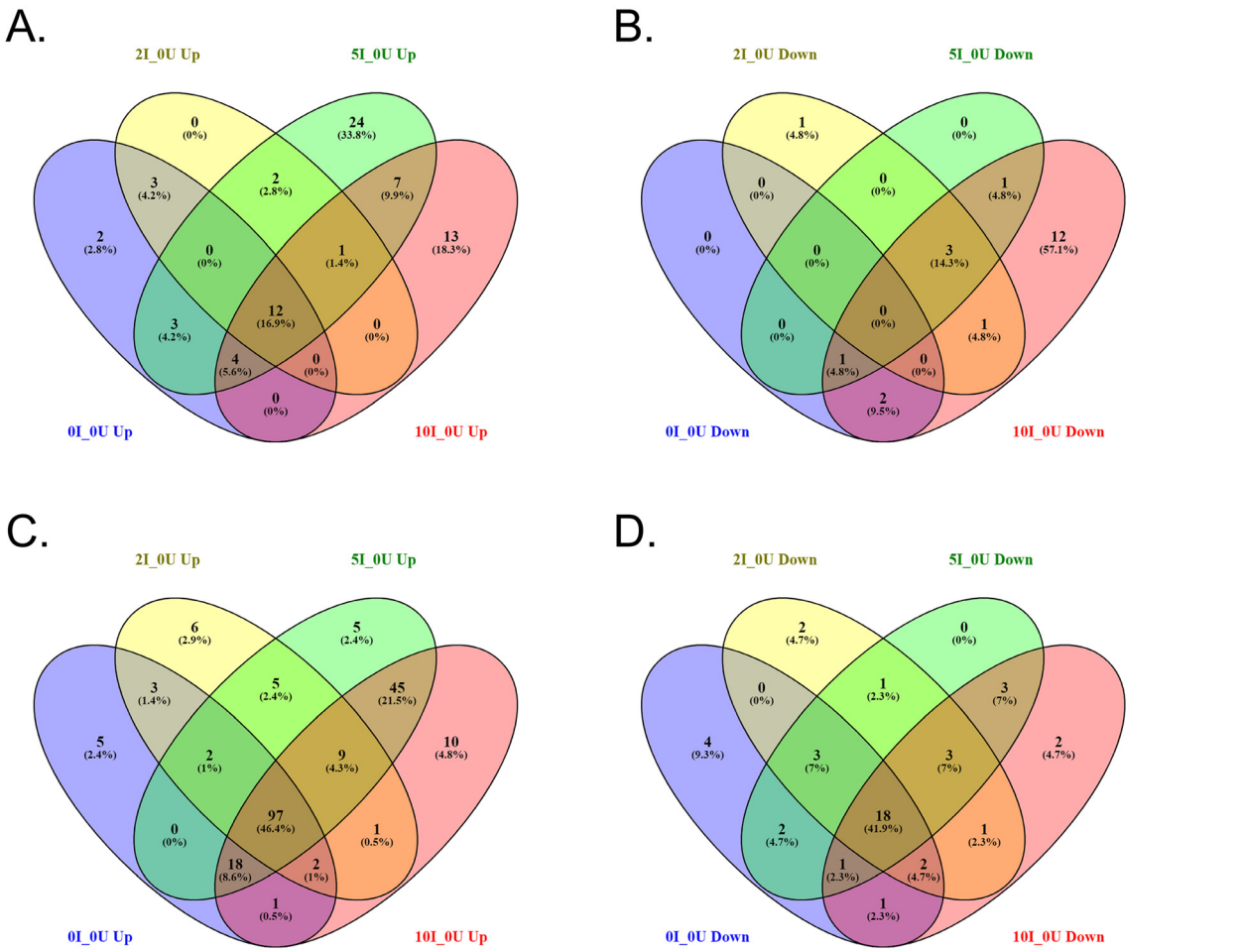

Fig. 8 Venn analysis of Reactome pathways identified by DAVID in the cecum and DC of *Cr*-infected mice compared with uninfected mice fed the basal diet. Pathways Venn analysis of upregulated (A, C) or downregulated (B, D) (≥1.5-fold) of *Cr*-infected mice fed different levels of VF compared with uninfected mice fed the basal diet in the cecum (A, B) and or DC (C, D). ≥1.5-fold, FDR adjusted $p < 0.05$, $n = 5$ per group.

involved in "Immune System", "Cytokine Signaling in Immune System", "Neutrophil Degranulation" and "Adaptive Immune System" by VF in infected animals (ESI Table 7†). In infected animals, the number of genes and statistical significance of the genes in the pathway increased in a largely dose-dependent manner; however, the enrichment scores were all similar.

ESI Tables 10 and 11† contain the summary of all identified KEGG pathways for the cecum and DC, respectively. The mmu04668:TNF signaling pathway was selectively enriched in the cecum (5I_0I, 5.9 fold, $p = 1.38 \times 10^{-2}$; 10I_0I, 7.9 fold, $p = 1.65 \times 10^{-9}$) and the DC (5I_0I, 6.7 fold, $p = 9.50 \times 10^{-4}$; 10I_0I, 6.0 fold, $p = 2.50 \times 10^{-2}$). Similarly, the mmu04657:IL-17 signaling pathway was selectively enriched in the cecum (10I_0I, 5.1-fold, $p = 2.43 \times 10^{-3}$) and in the DC (5I_0I, 9.1-fold, $p = 4.46 \times 10^{-5}$; 10I_0I, 6.5-fold, $p = 3.89 \times 10^{-2}$). In the cecum, another pathway of note, mmu00830:Retinol metabolism, was identified as a commonly downregulated pathway in the 5I_0I (10.1-fold, $p = 3.94 \times 10^{-4}$) and 10I_0I (5.9-fold, $p = 7.81 \times 10^{-6}$) comparisons. This did not occur in the DC.

Detailed correlation network parameters between the cecal microbiome and differentially expressed genes in the distal colon in infected animals can be found in ESI Table 12.† A network of genera that were significantly correlated with genes within the distal colon of infected mice fed 0, 2, 5 and 10% VF can be seen in Fig. 9, panels A, B, C and D, respectively. *Citrobacter*-associated genes are shown in yellow. The analysis of DEG in distal colon 0I_0U using Reactome "Cytokine Signaling in Immune System" pathway (A), yielded a network of 11 bacteria and 45 genes and *Citrobacter* was associated with 7 genes, including *Il36g* ($r = 1.00$) and *Il21* ($r = 0.802$). *Ifng* (not shown) was also associated with *Citrobacter* at a $p < 0.05$, but the regression coefficient did not reach the established cutoff value ($r = 0.747$). *Defluviitaleaceae UCG-011* was associated with 6 genes including *Ifng* ($r = 0.870$) and *Tnf* ($r = 0.869$). For the 2I_0U comparison (B), there were 16 bacteria associated with 48 genes. *Citrobacter* was associated with 5 genes including *Il21* ($r = 0.829$). *Ifng* (not shown) was not associated with *Citrobacter* at a $p > 0.05$ ($r = 0.543$). The bacteria classified as *Unknown Family (RF39)* is associated with 15 genes includ-

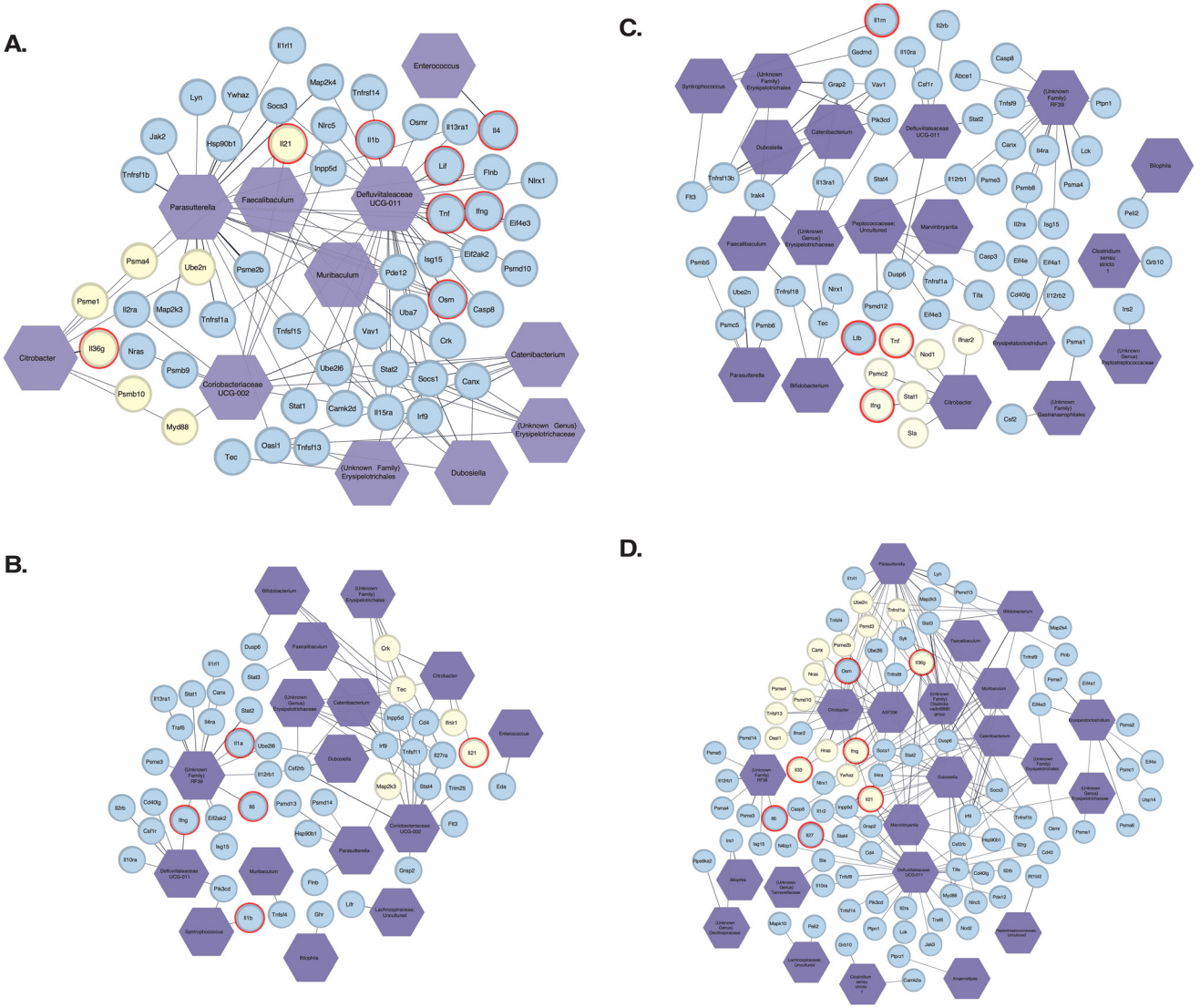

Fig. 9 Network of genera that were significantly correlated with cytokine signaling-related genes within the distal colon of infected mice fed 0% (A), 2% (B), 5% (C) and 10% (D) VF. *Citrobacter*-associated genes are shown in yellow and edge thickness corresponds to the strength of the correlation (FDR adjusted $p < 0.05$, $n = 5$ per group). Cytokines are outlined in red.

ing *Il1a* ($r = 0.822$), *Il6* ($r = 0.854$) and *Ifng* ($r = 0.831$). The bacteria *Defluviitaleaceae UCG-011* was associated with 6 genes including *Ifng* ($r = 0.886$). *Syntrophococcus* was associated with 2 genes including *Il1b* (0.832).

For the 5I_0U comparison (C), there were 18 bacteria associated with 57 genes. *Citrobacter* was associated with 7 genes, including *Ifng* ($r = 0.886$) and *Tnf* ($r = 0.831$). *Il21* (not shown) was also associated with *Citrobacter* at a $p < 0.05$, but the regression coefficient did not reach the established cutoff value ($r = 0.714$). For the 10I_0U comparison (D), there were 23 bacteria associated with 81 genes. *Citrobacter* was significantly ($r > 0.8$, FDR $p < 0.05$) associated with 16 genes including *Ifng* ($r = 0.829$), *Il21* ($r = 0.829$), *I33* ($r = 0.831$), and Il36g ($r = 0.886$). *ASF356* and *Dubosiella* were also associated with *Ifng* ($r = 0.829$) and ($r = 0.831$) respectively. The bacteria annotated as *Unknown Family (RF39)* was significantly associated with 7 genes including *Il6* ($p = 0.810$). *Defluviitaleaceae UCG-011* was associated with 13 genes including *Il27*.

Discussion

The results presented here demonstrate that feeding mice VF, a phosphorylated and crosslinked potato starch that is 85% fiber by the AOAC 991.43 method (Ingredion technical specification sheet), in the context of a TWD,[27] had significant effects on the microbiome, gene expression, and caused increased *Cr* colonization and pathology. The levels of VF consumed by the mice is approximately equivalent to a human consuming between 8 and 45 g of RS per day using the method of Whelan based on energy consumption. This is relevant to a typical human diet, as according to the 21 CFR 101.12, the Reference

Amount Customarily Consumed (RACC) per eating occasion for starches, including potato starches, is 10 g. The actual amount of VF consumed by the general public is unknown since VF is added to products to enhance the fiber content. Others, however, have used similar doses in their studies by adding VF to nutrition bars or baked goods. Human subjects were fed 2, 21 or 30 g of VF per day, with the higher doses reducing post-prandial glucose and insulin responses.[86] A similar effect on post-prandial glucose and insulin responses was observed in human subjects fed 25 g of VF[87] but not in a third study where human subjects were fed 10 or 20 g of VF.[88]

We had previously found that RPS, an unmodified starch, caused a dose-dependent decrease in alpha-diversity that was due in part to a very large increase in the *Lachnospiraceae NK4A136 group.*[46,47] In this study, decreased alpha-diversity, as measured by the Shannon Index, was observed only in mice fed the 10% VF diet, and is consistent with the other studies where feeding RS decreased alpha-diversity in rodents[6,21,89–91] and pigs,[92–94] but was unaffected by *Cr* infection. Feeding VF, a phosphorylated, crosslinked RS, had a less pronounced effect on beta-diversity compared with unmodified RPS, with differences only observed in mice fed the 5% and 10% VF diets compared with the basal diet (Fig. 5 and ESI Fig. 2A, B†). *Cr* infection, however, did result in further separation into distinct groups of infected mice fed 5% and 10% VF, indicating that infection itself affected beta-diversity. These results suggest that modification of starch by phosphorylating and crosslinking reduced the ability of the starch to affect changes to the microbiome diversity and lends further evidence to the concept that the fine structure of fibers and starches can affect the ability of the microbiota to utilize a particular starch or fiber.[15,17]

Feeding RPS to mice and rats caused an increase in colon and cecum weight.[46,95,96] A modest increase in colon/body weight ratio was observed in uninfected mice fed the 10% VF diet (Fig. 1B). *Cr* infection induces crypt hyperplasia and thickening of the colon.[97] We observed a dose-dependent effect of dietary VF on the % colon/body weight ratio in *Cr*-infected mice that was also reflected in an increase in mucosa thickness with increasing dietary VF (Fig. 3A). %Cecum/body-weight ratios increased with increasing dietary VF in both uninfected and infected mice with the effect slightly more pronounced in infected mice fed the 2% and 5% but not the TWD or 10% VF diets. The increase in cecum weights regardless of infection status likely reflects increased levels of undigested material reaching the cecum with increasing dietary VF for subsequent fermentation by commensal bacteria. Others have also observed enlargement of the cecum in rodents fed RS[5,20,21,89] including VF.[98]

Feeding VF led to specific changes to the microbiota at the genus level. These changes were most prominent in mice fed the 10% VF diet. About equal numbers of genera increased or decreased in relative abundance in response to feeding VF in both uninfected and infected mice and contrasts to our results with RPS, where only a few genera increased in abundance in response to feeding RPS. Notably, while the RA of *Lachnospiraceae NK4A136 group* went from approximately 10% to 50% relative abundance in a graded manner in response to increasing dietary RPS,[46] that was partially blunted by infection,[47] the increase in VF fed mice was much less (12%) and similar in magnitude in both uninfected and infected mice, suggesting that this genus cannot utilize the cross-linked and phosphorylated VF to the same extent as the native RPS and is not further affected by *Cr* infection.

The TWD is a low-fiber diet containing 3% cellulose as the sole fiber source and adding RS increases the effective fiber concentration providing a substrate for fermentation by commensal microbes. We previously showed that mice fed the TWD had decreased initial colonization by *Cr* compared with RPS-fed mice, and feeding RPS increased colonization by *Cr* that led to increased pathology in mice fed a diet containing 10% RPS.[47] Similar results were found in this study, with increased colonization in mice fed a diet containing 10% VF compared with the TWD and increased pathology in mice fed the 5% and 10% VF diets. Thus, feeding two different RS led to aggravated *Cr* infections, suggesting that feeding different RS in general may lead to increased colonization by *Cr*. Consistent with our results, compared with mice fed a purified high-fat low-fiber Western-style diet, feeding a high-fiber chow diet increased *Cr* colonization.[35] Furthermore, mice fed a chow diet or a semi-synthetic diet (5% cellulose) containing 10% inulin had increased colonization by *Cr* and increased worm burden by the cecum-dwelling *Trichuris muris* compared with mice fed the semi-synthetic diet alone, but not another small-intestine-dwelling nematode, *Heligmosomoides polygyrus*[99] indicating the effect may be restricted to the cecum and colon where fermentation occurs. Another study comparing feeding a chow-based diet with a purified AIN-93G diet found altered villi and crypt lengths, altered epithelial turnover, barrier function and microbiome in the AIN-93G-fed mice.[100] Together these results indicate that diets rich in fiber or RS increase susceptibility to some pathogens that infect the large intestine, and have implications when considering the role played by diet in resistance to food-borne pathogens. *In toto*, the results of these various studies indicate that use of purified diets may introduce a bias that needs to be considered when designing and analyzing experiments.

The mechanism by which dietary fiber and RS are altering susceptibility to *Cr* is not clear. Administration of IL22, important for clearance of *Cr*, did not restore resistance to *Cr* colonization in mice fed a semi-synthetic diet containing inulin, suggesting a non-immune mechanism may be responsible.[99] This could be related to specific bacteria and their metabolites produced during the time of infection in response to a fermentable substrate. The microbiome is known to influence resistance to *Cr* infection.[101] We observed some evidence of this in our study through altered abundances of other genera that have been associated with greater or lesser degree of *Cr* infection (Fig. 6 and ESI Table 2†). For example, the absence of *Turicibacterales* was recently shown to be associated with more severe *Cr*-induced disease.[64] *Turicibacter* RA was decreased in mice fed RPS[47] or VF in this study with the greatest decrease

seen in mice fed diets with 10% added RS where maximum increased colonization and pathology was observed. *Blautia* RA was reduced with increasing VF only in *Cr*-infected mice. *Blautia* has been shown to suppress *Vibrio cholera*[102] and *Cr* colonization[103] and to improve DSS-induced colitis.[104] *Parasutterella* and *Erysipelatoclostridium* genera RA also significantly increased in a dose-dependent manner, and have been shown to increase in DSS-treated colitis mice.[105] Increases in *Bifidobacterium* and *Faecalibacterium* and a decrease in *Clostridium sensu stricto 1* were also in agreement with previous findings regarding higher susceptibility to *Cr* infection.[99] Thus, specific dietary-induced changes in the microbiome likely contributed to the increased colonization and pathology in VF-fed mice.

Others have reported metabolic changes induced by consumption of RS and by *Cr* infection that were predictive of increased colonization.[106,107] RS and dietary fiber are degraded to generate mono- and di-saccharides which can then be fermented by gut commensal bacteria to produce a wide variety of metabolites including SCFAs and succinate that can regulate *Cr* colonization and pathology. High levels of butyrate and acetate have been shown to increase resistance to *Cr* infection.[42,108] In closely related *E. coli*, however, butyrate markedly enhanced the expression of virulence-associated genes[109] and the effect of butyrate on *Cr* resistance may be dose dependent. Feeding mice the 5% or 10% VF diets increased butyrate levels, but the levels were far below those associated with inhibition of *Cr.*[63] *Cr* has been shown to effectively use acetate as an energy source as well, and perhaps diets that promote acetate-producing bacteria could, in part, also be supporting the persistence of *Cr* infection.[110] Succinate is also a product of fermentation and can be used by the *Cr* gluconeogenic master regulator Cra to activate expression of the locus of enterocyte effacement required for pathogenicity.[111] Monosaccharides, which can be derived from RS and dietary fiber, are likely to be important for early colonization as both *Cr* and *E. coli* exhibited optimal growth on monosaccharides[112] and studies have shown that pathogenic *E. coli* prefer simple sugars for growth.[113,114] Thus, diets with added RS or fiber can be a source material for producing metabolites that can significantly alter *Cr* colonization and pathology.

A number of cytokines and chemokines that are important for control of *Cr* infections and inflammation, including Ifng,[115] *Il-17a*, *Il17c*, *Il21* and *Il*22,[116] had their expression modified by feeding VF. In general, there were higher levels of gene expression associated with Th1, Th17 and inflammation in the DC where *Cr* replication predominates later in the infection cycle compared with the cecum. Interferon-g is the principal driver of Th1 responses[117] and is critical for mediating the immune response to *Cr.*[115] In the present experiment, *Ifng* was not significantly upregulated by increasing dietary VF in the cecum of infected mice but *Ifng* was significantly induced by infection (0I_0U, 350.7-fold, $p = 4.94 \times 10^{-5}$) to higher levels in the DC than in cecum. VF at the 2%, 5% and 10% levels compared with the 0U group progressively increased infection-induced expression up to 1064.2-fold ($p = 4.95 \times 10^{-7}$, Table 4).

A pattern of expression similar to *Ifng* was observed for *IL17a* and *Il17c* in the DC (Table 4) but not the cecum (Table 3). In the cecum, *Il17a* was only upregulated in the 10% VF treatment groups *versus* the 0U group (46.6, $p < 2.02 \times 10^{-2}$), and this correlated with the higher levels of *Cr* in the cecum in mice fed the 10% VF diet, but neither diet nor infection affected *IL17c* expression. In DC, *Il17a* mRNA was significantly induced by infection (14.3-fold, $p = 1.56 \times 10^{-4}$). The 2%, 5% and 10% VF were similarly effective at increasing infection-induced expression. Feeding VF, but not the basal diet, induced similar levels of *Il17c* in the DC of infected mice compared to the 0U group (6.3-fold, $p = 9.46 \times 10^{-4}$, 5.1-fold, $p = 3.42 \times 10^{-3}$, and 5.0-fold, $p = 4.00 \times 10^{-3}$ for the 2I_0U, 5I_0U and 10I_0U comparisons, respectively). Taken together with KEGG analyses showing enrichment of the mmu04657:IL-17 signaling pathway in 5I_0I and 10I_0I comparisons, infection induced a Th17 response, and this response was enhanced by VF, but the effect was only partially dose dependent.

Interleukin-22 is produced by ILC3 cells, NK cells and TH17 cells[118,119] and is important for controlling *Cr* infections.[116] It is a positive regulator of inflammation and is associated with Th1[120] and Th17-responses.[121] Unlike our previous experiment, *Il22* was not consistently regulated by VF in the cecum and one of its receptors, *Il22ra2*, was only significantly downregulated in the 5I_0U and 10I_0U groups (−5.2-fold, $p = 2.27 \times 10^{-6}$, and −14.2-fold, $p = 6.43 \times 10^{-14}$) compared with 0I_0U. However, in the DC, *Il22* was upregulated and *Il22ra2*, downregulated in all infected *versus* uninfected control comparisons. Il22ra2 is a decoy receptor and acts as an Il22 receptor antagonist[122] and the expected biological response would be to increase the local production and activity of Il22 in both tissues.

Other cytokines and chemokines that are important for controlling *Cr* infections and inflammation had their expression altered by feeding VF. *Cxcl9* and *Cxcl10* and *Cxcl1*, all induced by Ifn-g,[123] are chemoattractants for cells expressing CXCR3, including neutrophils that are important for control of *Cr* infections[124] and *Cxcl9* expressed antibacterial activity against *C. rodentium.*[125] In cecum, VF increased the expression of the chemokines, chemokine (C-X-C motif) ligand 9 (*Cxcl9*), *Cxcl10* in the I_0U comparisons in a dose-dependent fashion. The expression of *Cxcl9* was significantly increased in the 5I_0I and10I_0I comparisons. *Cxcl10* was significantly increased in the 10I_0I comparison. In DC, VF increased the expression of *Cxcl9* and *Cxcl10* in the I_0U comparisons in a dose-dependent fashion. The expression of *Cxcl11* was significantly ($p = 4.7 \times 10^{-2}$) increased 3.2-fold in the 10I_0I comparison.

Nitric oxide synthase (*Nos2*) is produced primarily by LPS and IFN-γ-stimulated macrophages in the mouse and its product, nitric oxide, possesses anti-bacterial properties.[126] In the DC, *Nos2* expression increased in a pure dose-dependent response from 337.8 to 558.2-fold. In the cecum, *Nos2* also increased in a pure dose-dependent response but was less pronounced than in the DC, again reflecting the higher *Cr* burden in the DC late in the infection cycle. Overproduction of nitric

oxide can lead to gross cellular and tissue damage and may have contributed to the increased colon pathology in the 5% and 10% VF mice. At high levels it also inhibits T-cell function (apoptosis of Th1 cells, and reduction of Th17 differentiation).[127,128] It is tempting to speculate that overproduction of Nos2 in the DC contributes to the enhanced pathology seen in response to increasing levels of VF in our model.

We observed increased colonic mucosa hyperplasia and pathology in *Cr*-infected mice fed 5% and 10% dietary VF. Inflammation can contribute to tissue pathology and multiple markers of inflammation were also found to be differentially expressed due to infection in the cecum (Table 3) and DC (Table 4) but the gene expression changes were larger in the distal colon where *Cr* replication predominates later in the infection cycle. Changes in inflammatory gene expression due to feeding VF were predominately found in the DC with the exceptions of *Il1b* and *Tnf* whose expression was modified by VF in the cecum. In the DC, the proinflammatory cytokines, *Il1b*, *Il6* and *Il36g* were increased by infection (0I_0U) 9.4 ($p = 5.48 \times 10^{-18}$), 5.6 (not significant) and 453.7-fold ($p = 3.02 \times 10^{-5}$), respectively. A modest effect of feeding VF was observed on *Il1b* and *Il6* expression in mice fed the 5% or 10% VF diets. Although greatly elevated by infection in the DC compared with the cecum, *Tnf* expression in the DC was not affected by feeding VF. However, a KEGG analysis identified the mmu04668:TNF signaling pathway as being enriched in the 5I_0I and 10I_0I comparisons in both the cecum and DC, suggesting that feeding VF did affect the TNF pathway in both the cecum and DC. Il36g belongs to the interleukin 1 superfamily and is expressed predominantly by pathogen-exposed epithelial cells.[129] Its expression was highly upregulated in the I_0U comparisons that increased in a dose-dependent manner but no significant differences were seen in the I_0I comparisons (Table 4). The Interleukin 1 receptor, type II (*Il1r2*) was upregulated in a largely dose-dependent fashion in DC. It was significantly upregulated in 5I_0I and 10I_0I comparisons. *Il1r2* is a decoy receptor for *IL-1a* and *IL-1b*, limiting their biological activity.[130] Higher levels of *Il1r2* have been associated with innate immune dysfunction and increased pathogenicity of bacterial infections in mice and humans.[131]

Fecal lipocalin 2 (*Lcn2*/NGAL), neutrophil-derived calprotectin (S100a9) and calprotectin L (*S100a8*) are fecal markers of inflammation.[132,133] In the cecum, *Lcn2* and *S100a9* were significantly upregulated in the 5I_0U (3.0 and 9.6-fold), 10I_0U (3.3 and 12.9-fold), comparisons (Table 3) but no significant differences were seen in the I_0I comparisons. In the DC, Lcn2 was upregulated by infection (0I_0U) to a much larger extent than in the cecum and was further induced by VF in the 5I_0U and 10I_0U comparisons with significance also achieved in the 5I_0I and 10I_0I comparisons, indicating that feeding VF enhanced expression within infected animals. Both *S100a8* and *S100a9* expression were dramatically upregulated by infection in the DC. *S100a9* expression was also increased in the 5I_0I and 10I_0I comparisons indicating that feeding VF increased expression further in the DC (Table 4) and correlates with increased *Cr* burden. Taken together, the evidence suggests that higher doses (5% and 10%) of VF exacerbate inflammation in the cecum and DC of *Cr*-infected mice and correlates with increased pathology in the DC in mice fed the 5% and 10% VF diets.

Signaling through the AhR pathway is critical for control of *Cr* infections.[134] *Cyp1a1*, an AhR-targeted gene,[135] whose expression is downregulated by LPS and TNF *via* NF-Kb1 binding to the *Cyp1a1* promoter region,[136] was downregulated in cecum and DC in uninfected and infected animals, in a dose-dependent fashion suggesting that inflammation reduced signaling through AhR. In the intestine, genetic ablation of AhR[137] or the lack of AhR ligands[138] compromises the maintenance of intraepithelial lymphocytes (IELs) and the control of the microbial load and composition resulting in heightened immune activation and increased vulnerability to epithelial damage.

To further explore the gene expression results, pathway analyses were performed. Ninety-seven commonly upregulated pathways were identified by the DAVID Analysis of Reactome Pathways for the DC including "Immune System", "Cytokine Signaling in Immune System", "Neutrophil Degranulation" and "Adaptive Immune System" in infected animals fed different levels of VF compared with the 0U group (ESI Table 7†). The number of genes and statistical significance of the genes in the pathways increased in a largely dose-dependent manner; however, the enrichment scores were all similar. Looking at the top 20 most highly significant Reactome pathways within the four I_0U comparisons in the DC, the number of pathways associated with the cell cycle increased with the level of dietary VF from 3, 3, 11 and 11 in the 0I_0U, 2I_0U, 5I_0U and 10I_0U comparisons, respectively (ESI Table 9†). A more detailed analysis of genes associated with the cell cycle is also summarized in ESI Table 9.† There was a dose-dependent increase in upregulated genes associated with the cell cycle in the four I_0U comparisons but the differences between the infected groups was not significant. The increase in genes associated with the cell cycle correlates with increased hyperplasia in infected mice fed the 5 and 10% VF diets. Another Reactome pathway enriched by *Cr* infection in DC of animals was the R-MMU-191273~Cholesterol biosynthesis. In DC, we found a 4.1, 3.9, 3.4 and 3.4 fold-enrichment for the 0I_0U, 2I_0U, 5I_0U and 10I_0U comparisons, respectively (ESI Table 7†). Cholesterol is a component of biological membranes and has been shown to be important for innate immunity.[107] Previous experiments demonstrated increased cholesterol biogenesis in the colon-derived epithelial cells of *Cr*-infected animals.[106,139]

In our studies, Venn analysis of the DC DAVID Analysis of Reactome pathways revealed an increase in 21 genes (*Ndc1*, *Ranbp2*, *Sc13*, *Pfkfb4*, *Tpi1*, *Np107*, *Pfkfb3*, *Nup210*, *Pgam1*, *Bpgm*, *Nup160*, *Hk2*, *Pgm2l1*, *Np93*, *Hk3*, *Pkm*, *Nup50*, *Pk1*, *Gapdh*, *Pfkp*, *Nup37*) involved in R-MMU-70171~Glycolysis exclusively in the 10I_0U group (ESI Table 7†). Various sugar transporters *Slc2a1* (galactose, glucose, mannose), *Slc5a9* (fructose, glucose mannose) *Slc45a3* (glucose, sucrose), were

also upregulated in the10I_0U group. Previous studies have demonstrated increased aerobic glycolysis and *Slc5a9* expression in colon-derived epithelial cells of *Cr*-infected animals.[139] Unlike the latter study, we did not find decreased TCA cycle by Reactome mining, and no genes involved in the TCA cycle were significantly down regulated in the 10I_0U group. Although glycolysis favors the growth of bacteria, including *Cr*, it also promotes TH1[140] and TH17[141]-type responses.

As expected, the analysis of DEG in distal colon using Reactome "Cytokine Signaling in Immune System" pathway yielded an increasing number of bacteria (11, 16, 18) associated with increasing number of genes (45, 48, 57) in the 0I_0U, 2I_0U, 5I_0U and 10I_0U groups respectively. *Citrobacter* was associated with 7, 5, 7 and 16 genes in the 0I_0U, 2I_0U, 5I_0U and 10I_0U groups, respectively. Proinflammatory cytokine associations increased with dose; 0I_0U (*l36g*, *Il21*), 2I_0U (*Il21*), 5I_0U (*Ifng*, *Tnf*) and 10I_0U (*Ifng*, *Il21*, *Il33*, *Il36g*); although *Ifng* was only significant in the 5I_0U and 10I_0U comparisons. However, *Ifng* was significantly correlated to *Defluviitaleaceae UCG-011*, in the 0I_0U and 2I_0U comparisons. Recently, *Defluviitaleaceae UCG011* demonstrated proinflammatory properties. Studies have shown a positive correlation between higher levels of *Defluviitaleaceae UCG011* and the severity of DSS-induced colitis in mice[142] and pathology of human Crohn's disease[143] and a negative correlation with fecal butyric acid levels in rats.[144]

Additionally, *Ifng* was also correlated with *ASF356* and *Dubosiella* in the 10I_0U comparisons. *Il21* was associated with *Citrobacter* at all doses except 5I_0U where it almost reached the cutoff threshold (0.714). This relationship (between *Il-21* and dose of VF) seems paradoxical given that, *Il-21*, in conjunction with Ifn-γ, is important for the generation of secondary immune responses to *Cr.*[145]

Conclusions

Resistant starches have been promoted as a source of dietary fiber and the need to increase fiber in the diet has led to more RS being incorporated into food products. We demonstrated here that a commercially used RS4 derived from potato starch, VF, can increase colonization and colon pathology induced by a *Cr* infection.

Our finding of increased colonization of *Cr* in animals fed 10% VF provides further evidence that consumption of resistant starches promotes colonization. The effect of VF is not due to an impaired Th1/Th17 response to infection which, in general, was increased with increasing dietary VF compared with uninfected mice fed the basal diet. We also observed changes in the RA of specific genera, including *Blautia* and *Turicibacter* that confer resistance to *Cr* infection.[64,103] Thus, increased colon pathology is likely related to both specific changes to the microbiome and the heightened inflammatory response observed in mice fed the 5% and 10% VF diets.

Abbreviations

Cr	Citrobacter rodentium
DC	Distal colon
DF	Dietary fiber
HFD	High fat diet
NHANES	National Health and Nutrition Examination Survey
RS	Resistant starch
RPS	Resistant potato starch
SCFAs	Short chain fatty acids
Slc	Solute carrier family
TWD	Total Western diet
VF	Versafibe 1490™

Author contributions

AS and HD conceived and designed this experiment and supervised all experimental works. AS, EP, LC, and HD performed experiments. AS, CC, JR and HD performed data analysis. AS, EP, and HD drafted the manuscript. AS, EP, and HD helped to revise the manuscript. All authors have read and approved the final manuscript.

Institutional review board

All animal procedures were performed in accordance with the Guidelines for Care and Use of Laboratory Animals and approved by the USDA/ARS Beltsville Area Institutional Animal Care and Use Committee (Protocol 22-04).

Data availability

The FASTQ files with raw 16S data were submitted to the National Center for Biotechnology Information (NCBI) Sequence Read Archive (SRA) under Bioproject number PRJNA1141498, GEO Accession: GSE273638. The FASTQ files with raw data and the gene expression profiles were submitted to the National Center for Biotechnology Information (NCBI) Sequence Read Archive (SRA) under the BioProject ID: PRJNA1141498. Additional data supporting this article are available from the corresponding author upon reasonable request.

Conflicts of interest

The authors declare no conflicts of interest.

Acknowledgements

This work was supported by USDA ARS project 8040-53000-021-00D. The use of trade, firm, or corporation names in this publication (or page) is for the information and convenience

of the reader. Such use does not constitute an official endorsement or approval by the United States Department of Agriculture or the Agricultural Research Service of any product or service to the exclusion of others that may be suitable.

References

1 M. G. Sajilata, R. S. Singhal and P. R. Kulkarni, Resistant starch - A review, *Compr. Rev. Food Sci. Food Saf.*, 2006, **5**, 1–17.
2 M. M. Murphy, J. S. Douglass and A. Birkett, Resistant starch intakes in the United States, *J. Am. Diet. Assoc.*, 2008, **108**, 67–78.
3 K. Lange, F. Hugenholtz, M. C. Jonathan, H. A. Schols, M. Kleerebezem, H. Smidt, M. Müller and G. J. Hooiveld, Comparison of the effects of five dietary fibers on mucosal transcriptional profiles, and luminal microbiota composition and SCFA concentrations in murine colon, *Mol. Nutr. Food Res.*, 2015, **59**, 1590–1602.
4 A. Kaur, T. Chen, S. J. Green, E. Mutlu, B. R. Martin, P. Rumpagaporn, J. A. Patterson, A. Keshavarzian and B. R. Hamaker, Physical Inaccessibility of a Resistant Starch Shifts Mouse Gut Microbiota to Butyrogenic Firmicutes, *Mol. Nutr. Food Res.*, 2019, **63**, e1801012.
5 R. Nagata, N. Innami, S. Pelpolage, K. Shimada, H. Koaze, M. Tani, K. H. Han and M. Fukushima, Effects of Raw Potato Starch with High Resistant Starch Levels on Cecal Fermentation Properties in Rats, *J. Nutr. Sci. Vitaminol.*, 2019, **65**, S192–S195.
6 Y. Hu, R. K. Le Leu, C. T. Christophersen, R. Somashekar, M. A. Conlon, X. Q. Meng, J. M. Winter, R. J. Woodman, R. McKinnon and G. P. Young, Manipulation of the gut microbiota using resistant starch is associated with protection against colitis-associated colorectal cancer in rats, *Carcinogenesis*, 2016, **37**, 366–375.
7 J. M. Heo, A. K. Agyekum, Y. L. Yin, T. C. Rideout and C. M. Nyachoti, Feeding a diet containing resistant potato starch influences gastrointestinal tract traits and growth performance of weaned pigs, *J. Anim. Sci.*, 2014, **92**, 3906–3913.
8 D. Haenen, J. Zhang, C. Souza da Silva, G. Bosch, I. M. van der Meer, J. van Arkel, J. J. van den Borne, O. Pérez Gutiérrez, H. Smidt, B. Kemp, M. Müller and G. J. Hooiveld, A diet high in resistant starch modulates microbiota composition, SCFA concentrations, and gene expression in pig intestine, *J. Nutr.*, 2013, **143**, 274–283.
9 M. S. Hedemann and K. E. Bach Knudsen, Resistant starch for weaning pigs—Effect on concentration of short chain fatty acids in digesta and intestinal morphology, *Livest. Sci.*, 2007, **108**, 175–177.
10 X. Yang, K. O. Darko, Y. Huang, C. He, H. Yang, S. He, J. Li, J. Li, B. Hocher and Y. Yin, Resistant Starch Regulates Gut Microbiota: Structure, Biochemistry and Cell Signalling, *Cell. Physiol. Biochem.*, 2017, **42**, 306–318.
11 R. L. Hughes, W. H. Horn, P. Finnegan, J. W. Newman, M. L. Marco, N. L. Keim and M. E. Kable, Resistant Starch Type 2 from Wheat Reduces Postprandial Glycemic Response with Concurrent Alterations in Gut Microbiota Composition, *Nutrients*, 2021, **13**, 645.
12 J. H. Cummings, E. W. Pomare, W. J. Branch, C. P. Naylor and G. T. Macfarlane, Short chain fatty acids in human large intestine, portal, hepatic and venous blood, *Gut*, 1987, **28**, 1221–1227.
13 J. M. Wong, R. de Souza, C. W. Kendall, A. Emam and D. J. Jenkins, Colonic health: fermentation and short chain fatty acids, *J. Clin. Gastroenterol.*, 2006, **40**, 235–243.
14 S. M. Lancaster, B. Lee-McMullen, C. W. Abbott, J. V. Quijada, D. Hornburg, H. Park, D. Perelman, D. J. Peterson, M. Tang, A. Robinson, S. Ahadi, K. Contrepois, C. J. Hung, M. Ashland, T. McLaughlin, A. Boonyanit, A. Horning, J. L. Sonnenburg and M. P. Snyder, Global, distinctive, and personal changes in molecular and microbial profiles by specific fibers in humans, *Cell Host Microbe*, 2022, **30**, 848–862.
15 T. M. Cantu-Jungles, N. Bulut, E. Chambry, A. Ruthes, M. Iacomini, A. Keshavarzian, T. A. Johnson and B. R. Hamaker, Dietary Fiber Hierarchical Specificity: the Missing Link for Predictable and Strong Shifts in Gut Bacterial Communities, *mBio*, 2021, **12**, e0102821.
16 E. C. Deehan, C. Yang, M. E. Perez-Munoz, N. K. Nguyen, C. C. Cheng, L. Triador, Z. Zhang, J. A. Bakal and J. Walter, Precision Microbiome Modulation with Discrete Dietary Fiber Structures Directs Short-Chain Fatty Acid Production, *Cell Host Microbe*, 2020, **27**, 389–404.
17 H. Xu, N. A. Pudlo, T. M. Cantu-Jungles, Y. E. Tuncil, X. Nie, A. Kaur, B. L. Reuhs, E. C. Martens and B. R. Hamaker, When simplicity triumphs: niche specialization of gut bacteria exists even for simple fiber structures, *ISME Commun.*, 2024, **4**, ycae037.
18 B. R. Hamaker and Y. E. Tuncil, A perspective on the complexity of dietary fiber structures and their potential effect on the gut microbiota, *J. Mol. Biol.*, 2014, **426**, 3838–3850.
19 E. Ostrem Loss, J. Thompson, P. L. K. Cheung, Y. Qian and O. S. Venturelli, Carbohydrate complexity limits microbial growth and reduces the sensitivity of human gut communities to perturbations, *Nat. Ecol. Evol.*, 2023, **7**, 127–142.
20 D. A. Kieffer, B. D. Piccolo, M. L. Marco, E. B. Kim, M. L. Goodson, M. J. Keenan, T. N. Dunn, K. E. Knudsen, R. J. Martin and S. H. Adams, Mice Fed a High-Fat Diet Supplemented with Resistant Starch Display Marked Shifts in the Liver Metabolome Concurrent with Altered Gut Bacteria, *J. Nutr.*, 2016, **146**, 2476–2490.
21 J. Barouei, Z. Bendiks, A. Martinic, D. Mishchuk, D. Heeney, Y. H. Hsieh, D. Kieffer, J. Zaragoza, R. Martin, C. Slupsky and M. L. Marco, Microbiota, metabolome, and immune alterations in obese mice fed a high-fat diet containing type 2 resistant starch, *Mol. Nutr. Food Res.*, 2017, **61**, 1700184.
22 D. Chang, X. Hu and Z. Ma, Pea-Resistant Starch with Different Multi-scale Structural Features Attenuates the

Obesity-Related Physiological Changes in High-Fat Diet Mice, *J. Agric. Food Chem.*, 2022, **70**, 11377–11390.

23 C. P. Rosado, V. Rosa, B. Martins, A. Soares, A. Almo, E. Monteiro, A. Mulder, N. Moura-Nunes and J. B. Daleprane, Green banana flour supplementation improves obesity-associated systemic inflammation and regulates gut microbiota profile in high-fat diet-fed mice, *Appl. Physiol., Nutr., Metab.*, 2021, **46**, 1469–1475.

24 A. D. Benninghoff, K. J. Hintze, S. P. Monsanto, D. M. Rodriguez, A. H. Hunter, S. Phatak, J. J. Pestka, A. J. V. Wettere and R. E. Ward, Consumption of the Total Western Diet Promotes Colitis and Inflammation-Associated Colorectal Cancer in Mice, *Nutrients*, 2020, **12**, 544.

25 D. M. Rodriguez, K. J. Hintze, G. Rompato, A. J. V. Wettere, R. E. Ward, S. Phatak, C. Neal, T. Armbrust, E. C. Stewart, A. J. Thomas and A. D. Benninghoff, Dietary Supplementation with Black Raspberries Altered the Gut Microbiome Composition in a Mouse Model of Colitis-Associated Colorectal Cancer, although with Differing Effects for a Healthy versus a Western Basal Diet, *Nutrients*, 2022, **14**, 5270.

26 R. E. Ward, A. D. Benninghoff, B. J. Healy, M. Li, B. Vagu and K. J. Hintze, Consumption of the total Western diet differentially affects the response to green tea in rodent models of chronic disease compared to the AIN93G diet, *Mol. Nutr. Food Res.*, 2017, **61**, 1600720.

27 K. J. Hintze, A. D. Benninghoff and R. E. Ward, Formulation of the Total Western Diet (TWD) as a basal diet for rodent cancer studies, *J. Agric. Food Chem.*, 2012, **60**, 6736–6742.

28 C. Le Berre, S. Honap and L. Peyrin-Biroulet, Ulcerative colitis, *Lancet*, 2023, **402**, 571–584.

29 J. L. Jones, G. C. Nguyen, E. I. Benchimol, C. N. Bernstein, A. Bitton, G. G. Kaplan, S. K. Murthy, K. Lee, J. Cooke-Lauder and A. R. Otley, The Impact of Inflammatory Bowel Disease in Canada 2018: Quality of Life, *J. Can. Assoc. Gastroenterol.*, 2019, **2**, S42–S48.

30 N. Ekstedt, D. Jamioł-Milc and J. Pieczyńska, Importance of Gut Microbiota in Patients with Inflammatory Bowel Disease, *Nutrients*, 2024, **16**, 2092.

31 B. A. Vallance, C. Chan, M. L. Robertson and B. B. Finlay, Enteropathogenic and enterohemorrhagic Escherichia coli infections: emerging themes in pathogenesis and prevention, *Can. J. Gastroenterol.*, 2002, **16**, 771–778.

32 N. K. Petty, R. Bulgin, V. F. Crepin, A. M. Cerdeno-Tarraga, G. N. Schroeder, M. A. Quail, N. Lennard, C. Corton, A. Barron, L. Clark, A. L. Toribio, J. Parkhill, G. Dougan, G. Frankel and N. R. Thomson, The Citrobacter rodentium genome sequence reveals convergent evolution with human pathogenic Escherichia coli, *J. Bacteriol.*, 2010, **192**, 525–538.

33 A. P. Gobert, K. T. Wilson and C. Martin, Cellular responses to attaching and effacing bacteria: activation and implication of the innate immune system, *Arch. Immunol. Ther. Exp.*, 2005, **53**, 234–244.

34 J. W. Collins, K. M. Keeney, V. F. Crepin, V. A. Rathinam, K. A. Fitzgerald, B. B. Finlay and G. Frankel, Citrobacter rodentium: infection, inflammation and the microbiota, *Nat. Rev. Microbiol.*, 2014, **12**, 612–623.

35 J. An, X. Zhao, Y. Wang, J. Noriega, A. T. Gewirtz and J. Zou, Western-style diet impedes colonization and clearance of Citrobacter rodentium, *PLoS Pathog.*, 2021, **17**, e1009497.

36 P. Maattanen, E. Lurz, S. R. Botts, R. Y. Wu, C. W. Yeung, B. Li, S. Abiff, K. C. Johnson-Henry, D. Lepp, K. A. Power, A. Pierro, M. E. Surette and P. M. Sherman, Ground flaxseed reverses protection of a reduced-fat diet against Citrobacter rodentium-induced colitis, *Am. J. Physiol.: Gastrointest. Liver Physiol.*, 2018, **315**, G788–G798.

37 D. DeCoffe, C. Quin, S. K. Gill, N. Tasnim, K. Brown, A. Godovannyi, C. Dai, N. Abulizi, Y. K. Chan, S. Ghosh and D. L. Gibson, Dietary Lipid Type, Rather Than Total Number of Calories, Alters Outcomes of Enteric Infection in Mice, *J. Infect. Dis.*, 2016, **213**, 1846–1856.

38 M. S. Desai, A. M. Seekatz, N. M. Koropatkin, N. Kamada, C. A. Hickey, M. Wolter, N. A. Pudlo, S. Kitamoto, N. Terrapon, A. Muller, V. B. Young, B. Henrissat, P. Wilmes, T. S. Stappenbeck, G. Nunez and E. C. Martens, A Dietary Fiber-Deprived Gut Microbiota Degrades the Colonic Mucus Barrier and Enhances Pathogen Susceptibility, *Cell*, 2016, **167**, 1339–1353.

39 M. Neumann, A. Steimle, E. T. Grant, M. Wolter, A. Parrish, S. Willieme, D. Brenner, E. C. Martens and M. S. Desai, Deprivation of dietary fiber in specific-pathogen-free mice promotes susceptibility to the intestinal mucosal pathogen Citrobacter rodentium, *Gut Microbes*, 2021, **13**, 1966263.

40 J. A. Jiminez, T. C. Uwiera, D. W. Abbott, R. R. E. Uwiera and G. D. Inglis, Impacts of resistant starch and wheat bran consumption on enteric inflammation in relation to colonic bacterial community structures and short-chain fatty acid concentrations in mice, *Gut Pathog.*, 2016, **8**, 67.

41 J. A. Jiminez, T. C. Uwiera, D. W. Abbott, R. R. E. Uwiera and G. D. Inglis, Butyrate Supplementation at High Concentrations Alters Enteric Bacterial Communities and Reduces Intestinal Inflammation in Mice Infected with Citrobacter rodentium, *mSphere*, 2017, **2**, 67.

42 L. Osbelt, S. Thiemann, N. Smit, T. R. Lesker, M. Schroter, E. J. C. Galvez, K. Schmidt-Hohagen, M. C. Pils, S. Muhlen, P. Dersch, K. Hiller, D. Schluter, M. Neumann-Schaal and T. Strowig, Variations in microbiota composition of laboratory mice influence Citrobacter rodentium infection via variable short-chain fatty acid production, *PLoS Pathog.*, 2020, **16**, e1008448.

43 R. A. Rastall, M. Diez-Municio, S. D. Forssten, B. Hamaker, A. Meynier, F. J. Moreno, F. Respondek, B. Stahl, K. Venema and M. Wiese, Structure and function of non-digestible carbohydrates in the gut microbiome, *Benefic. Microbes*, 2022, **13**, 95–168.

44 L. B. Bindels, R. R. Segura Munoz, J. C. Gomes-Neto, V. Mutemberezi, I. Martínez, N. Salazar, E. A. Cody,

M. I. Quintero-Villegas, H. Kittana, C. G. de los Reyes-Gavilán, R. J. Schmaltz, G. G. Muccioli, J. Walter and A. E. Ramer-Tait, Resistant starch can improve insulin sensitivity independently of the gut microbiota, *Microbiome*, 2017, **5**, 12.

45 I. Martínez, J. Kim, P. R. Duffy, V. L. Schlegel and J. Walter, Resistant Starches Types 2 and 4 Have Differential Effects on the Composition of the Fecal Microbiota in Human Subjects, *PLoS One*, 2010, **5**, e15046.

46 A. D. Smith, C. Chen, L. Cheung, R. Ward, K. J. Hintze and H. D. Dawson, Resistant Potato Starch Alters the Cecal Microbiome and Gene Expression in Mice Fed a Western Diet Based on NHANES Data, *Front. Nutr.*, 2022, **9**, 782667.

47 A. D. Smith, C. Chen, L. Cheung and H. D. Dawson, Raw potato starch alters the microbiome, colon and cecal gene expression, and resistance to Citrobacter rodentium infection in mice fed a Western diet, *Front. Nutr.*, 2022, **9**, 1057318.

48 J. J. Kozich, S. L. Westcott, N. T. Baxter, S. K. Highlander and P. D. Schloss, Development of a dual-index sequencing strategy and curation pipeline for analyzing amplicon sequence data on the MiSeq Illumina sequencing platform, *Appl. Environ. Microbiol.*, 2013, **79**, 5112–5120.

49 A. D. Smith, C. Chen, L. Cheung, R. E. Ward, B. S. Jones, E. A. Pletsch and H. D. Dawson, A type 4 resistant potato starch alters the cecal microbiome and gene expression in mice fed a western diet based on NHANES data, *Food Funct.*, 2024, **15**, 3141–3157.

50 C. Quast, E. Pruesse, P. Yilmaz, J. Gerken, T. Schweer, P. Yarza, J. Peplies and F. O. Glockner, The SILVA ribosomal RNA gene database project: improved data processing and web-based tools, *Nucleic Acids Res.*, 2013, **41**, D590–D596.

51 R. C. Edgar, MUSCLE: multiple sequence alignment with high accuracy and high throughput, *Nucleic Acids Res.*, 2004, **32**, 1792–1797.

52 M. J. Anderson, A new method for non-parametric multivariate analysis of variance, *Austral Ecol.*, 2001, **26**, 32–46.

53 J. Oksanen, G. L. Simpson, F. G. Blanchet, R. Kindt, P. Legendre, P. R. Minchin, R. B. O'Hara, P. Solymos, M. H. H. Stevens, E. Szoecs, H. Wagner, M. Barbour, M. Bedward, B. Bolker, D. Borcard, G. Carvalho, M. Chirico, M. De Caceres, S. Durand, H. B. A. Evangelista, R. FitzJohn, M. Friendly, B. Furneaux, G. Hannigan, M. O. Hill, L. Lahti, D. McGlinn, M.-H. Ouellette, E. Ribeiro Cunha, T. Smith, A. Stier, C. J. F. Ter Braak and J. Weedon, vegan: Community Ecology Package, R package version 2.7-0, 2024, **https://github.com/vegandevs/vegan**.

54 B. H. McArdle and M. J. Anderson, Fitting Multivariate Models To Community Data: A Comment On Distance-Based Redundancy Analysis, *Ecology*, 2001, **82**, 290–297.

55 P. Martinez Arbizu, Pairwise Multilevel Comparison using Adonis, R package version 0.4, 2024, **https://github.com/pmartinezarbizu/pairwiseAdonis**.

56 R. Kolde, pheatmap: Pretty Heatmaps, R package version 1.0.12, 2019, **https://github.com/raivokolde/pheatmap**.

57 C. Galaxy, The Galaxy platform for accessible, reproducible and collaborative biomedical analyses: 2022 update, *Nucleic Acids Res.*, 2022, **50**, W345–W351.

58 P. Shannon, A. Markiel, O. Ozier, N. S. Baliga, J. T. Wang, D. Ramage, N. Amin, B. Schwikowski and T. Ideker, Cytoscape: a software environment for integrated models of biomolecular interaction networks, *Genome Res.*, 2003, **13**, 2498–2504.

59 H. D. Dawson, C. Chen, B. Gaynor, J. Shao and J. F. Urban Jr., The porcine translational research database: a manually curated, genomics and proteomics-based research resource, *BMC Genomics*, 2017, **18**, 643.

60 B. T. Sherman, M. Hao, J. Qiu, X. Jiao, M. W. Baseler, H. C. Lane, T. Imamichi and W. Chang, DAVID: a web server for functional enrichment analysis and functional annotation of gene lists (2021 update), *Nucleic Acids Res.*, 2022, **W216**, Web Server issue.

61 A. Fabregat, K. Sidiropoulos, G. Viteri, O. Forner, P. Marin-Garcia, V. Arnau, P. D'Eustachio, L. Stein and H. Hermjakob, Reactome pathway analysis: a high-performance in-memory approach, *BMC Bioinformatics*, 2017, **18**, 142.

62 Z. A. Bendiks, K. E. B. Knudsen, M. J. Keenan and M. L. Marco, Conserved and variable responses of the gut microbiome to resistant starch type 2, *Nutr. Res.*, 2020, **77**, 12–28.

63 A. D. Smith, C. Chen, L. Cheung, R. E. Ward, B. S. Jones, E. A. Pletsch and H. D. Dawson, A type 4 resistant potato starch alters the cecal microbiome and gene expression in mice fed a western diet based on NHANES data, *Food Funct.*, 2024, **15**, 3141–3157.

64 K. L. Hoek, K. G. McClanahan, Y. L. Latour, N. Shealy, M. B. Piazuelo, B. A. Vallance, M. X. Byndloss, K. T. Wilson and D. Olivares-Villagómez, Turicibacterales protect mice from severe Citrobacter rodentium infection, *Infect. Immun.*, 2023, **91**, e0032223.

65 L. A. Zenewicz, X. Yin, G. Wang, E. Elinav, L. Hao, L. Zhao and R. A. Flavell, IL-22 deficiency alters colonic microbiota to be transmissible and colitogenic, *J. Immunol.*, 2013, **190**, 5306–5312.

66 N. Burger-van Paassen, L. M. Loonen, J. Witte-Bouma, A. M. Korteland-van Male, A. C. de Bruijn, M. van der Sluis, P. Lu, J. B. Van Goudoever, J. M. Wells, J. Dekker, I. Van Seuningen and I. B. Renes, Mucin Muc2 deficiency and weaning influences the expression of the innate defense genes Reg3β, Reg3γ and angiogenin-4, *PLoS One*, 2012, **7**, e38798.

67 D. C. Propheter, A. L. Chara, T. A. Harris, K. A. Ruhn and L. V. Hooper, Resistin-like molecule beta is a bactericidal protein that promotes spatial segregation of the microbiota and the colonic epithelium, *Proc. Natl. Acad. Sci. U. S. A.*, 2017, **114**, 11027–11033.

68 J. V. Weinstock and D. E. Elliott, Helminth infections decrease host susceptibility to immune-mediated diseases, *J. Immunol.*, 2014, **193**, 3239–3247.

69 G. Lamprecht, J. Schaefer, K. Dietz and M. Gregor, Chloride and bicarbonate have similar affinities to the intestinal anion exchanger DRA (down regulated in adenoma), *Pfluegers Arch.*, 2006, **452**, 307–315.
70 P. G. Woodruff, H. A. Boushey, G. M. Dolganov, C. S. Barker, Y. H. Yang, S. Donnelly, A. Ellwanger, S. S. Sidhu, T. P. Dao-Pick, C. Pantoja, D. J. Erle, K. R. Yamamoto and J. V. Fahy, Genome-wide profiling identifies epithelial cell genes associated with asthma and with treatment response to corticosteroids, *Proc. Natl. Acad. Sci. U. S. A.*, 2007, **104**, 15858–15863.
71 S. R. Evans, W. B. Thoreson and C. L. Beck, Molecular and functional analyses of two new calcium-activated chloride channel family members from mouse eye and intestine, *J. Biol. Chem.*, 2004, **279**, 41792–41800.
72 K. A. Thomsson, J. M. Holmén-Larsson, J. Angström, M. E. Johansson, L. Xia and G. C. Hansson, Detailed O-glycomics of the Muc2 mucin from colon of wild-type, core 1- and core 3-transferase-deficient mice highlights differences compared with human MUC2, *Glycobiology*, 2012, **22**, 1128–1139.
73 T. Pelaseyed, J. H. Bergström, J. K. Gustafsson, A. Ermund, G. M. Birchenough, A. Schütte, S. van der Post, F. Svensson, A. M. Rodríguez-Piñeiro, E. E. Nyström, C. Wising, M. E. Johansson and G. C. Hansson, The mucus and mucins of the goblet cells and enterocytes provide the first defense line of the gastrointestinal tract and interact with the immune system, *Immunol. Rev.*, 2014, **260**, 8–20.
74 P. C. Kashyap, A. Marcobal, L. K. Ursell, S. A. Smits, E. D. Sonnenburg, E. K. Costello, S. K. Higginbottom, S. E. Domino, S. P. Holmes, D. A. Relman, R. Knight, J. I. Gordon and J. L. Sonnenburg, Genetically dictated change in host mucus carbohydrate landscape exerts a diet-dependent effect on the gut microbiota, *Proc. Natl. Acad. Sci. U. S. A.*, 2013, **110**, 17059–17064.
75 G. Huet, I. Kim, C. de Bolos, J. M. Lo-Guidice, O. Moreau, B. Hemon, C. Richet, P. Delannoy, F. X. Real and P. Degand, Characterization of mucins and proteoglycans synthesized by a mucin-secreting HT-29 cell subpopulation, *J. Cell Sci.*, 1995, **108**(Pt 3), 1275–1285.
76 T. Kiwamoto, T. Katoh, M. Tiemeyer and B. S. Bochner, The role of lung epithelial ligands for Siglec-8 and Siglec-F in eosinophilic inflammation, *Curr. Opin. Allergy Clin. Immunol.*, 2013, **13**, 106–111.
77 F. Xiao, Q. Yu, J. Li, M. E. Johansson, A. K. Singh, W. Xia, B. Riederer, R. Engelhardt, M. Montrose, M. Soleimani, D. A. Tian, G. Xu, G. C. Hansson and U. Seidler, Slc26a3 deficiency is associated with loss of colonic HCO3 (-) secretion, absence of a firm mucus layer and barrier impairment in mice, *Acta Physiol.*, 2014, **211**, 161–175.
78 R. A. Forman, M. L. deSchoolmeester, R. J. Hurst, S. H. Wright, A. D. Pemberton and K. J. Else, The goblet cell is the cellular source of the anti-microbial angiogenin 4 in the large intestine post Trichuris muris infection, *PLoS One*, 2012, **7**, e42248.
79 Y. G. Alevy, A. C. Patel, A. G. Romero, D. A. Patel, J. Tucker, W. T. Roswit, C. A. Miller, R. F. Heier, D. E. Byers, T. J. Brett and M. J. Holtzman, IL-13-induced airway mucus production is attenuated by MAPK13 inhibition, *J. Clin. Invest.*, 2012, **122**, 4555–4568.
80 A. Saku, K. Hirose, T. Ito, A. Iwata, T. Sato, H. Kaji, T. Tamachi, A. Suto, Y. Goto, S. E. Domino, H. Narimatsu, H. Kiyono and H. Nakajima, Fucosyltransferase 2 induces lung epithelial fucosylation and exacerbates house dust mite-induced airway inflammation, *J. Allergy Clin. Immunol.*, 2019, **144**, 698–709.
81 M. A. Schumacher, C. Y. Liu, K. Katada, M. H. Thai, J. J. Hsieh, B. J. Hansten, A. Waddell, M. J. Rosen and M. R. Frey, Deep crypt secretory cell differentiation in the colonic epithelium Is regulated by sprouty2 and interleukin 13, *Cell. Mol. Gastroenterol. Hepatol.*, 2023, **15**, 971–984.
82 C. C. Lewis, B. Aronow, J. Hutton, J. Santeliz, K. Dienger, N. Herman, F. D. Finkelman and M. Wills-Karp, Unique and overlapping gene expression patterns driven by IL-4 and IL-13 in the mouse lung, *J. Allergy Clin. Immunol.*, 2009, **123**, 795–804.
83 C. Zeng, S. Vanoni, D. Wu, J. M. Caldwell, J. C. Wheeler, K. Arora, T. K. Noah, L. Waggoner, J. A. Besse, A. N. Yamani, J. Uddin, M. Rochman, T. Wen, M. Chehade, M. H. Collins, V. A. Mukkada, P. E. Putnam, A. P. Naren, M. E. Rothenberg and S. P. Hogan, Solute carrier family 9, subfamily A, member 3 (SLC9A3)/sodium-hydrogen exchanger member 3 (NHE3) dysregulation and dilated intercellular spaces in patients with eosinophilic esophagitis, *J. Allergy Clin. Immunol.*, 2018, **142**, 1843–1855.
84 K. S. Bergstrom, J. A. Guttman, M. Rumi, C. Ma, S. Bouzari, M. A. Khan, D. L. Gibson, A. W. Vogl and B. A. Vallance, Modulation of intestinal goblet cell function during infection by an attaching and effacing bacterial pathogen, *Infect. Immun.*, 2008, **76**, 796–811.
85 J. M. Chan, G. Bhinder, H. P. Sham, N. Ryz, T. Huang, K. S. Bergstrom and B. A. Vallance, CD4+ T cells drive goblet cell depletion during Citrobacter rodentium infection, *Infect. Immun.*, 2013, **81**, 4649–4658.
86 V. Gourineni, M. L. Stewart, M. L. Wilcox and K. C. Maki, Nutritional Bar with Potato-Based Resistant Starch Attenuated Post-Prandial Glucose and Insulin Response in Healthy Adults, *Foods*, 2020, **9**, 1679.
87 M. L. Stewart and J. P. Zimmer, A High Fiber Cookie Made with Resistant Starch Type 4 Reduces Post-Prandial Glucose and Insulin Responses in Healthy Adults, *Nutrients*, 2017, **9**, 237.
88 Y. Du, Y. Wu, D. Xiao, G. Guzman, M. L. Stewart, V. Gourineni, B. Burton-Freeman and I. Edirisinghe, Food prototype containing resistant starch type 4 on postprandial glycemic response in healthy adults, *Food Funct.*, 2020, **11**, 2231–2237.
89 F. Goldsmith, J. Guice, R. Page, D. A. Welsh, C. M. Taylor, E. E. Blanchard, M. Luo, A. M. Raggio, R. W. Stout,

D. Carvajal-Aldaz, A. Gaither, C. Pelkman, J. Ye, R. J. Martin, J. Geaghan, H. A. Durham, D. Coulon and M. J. Keenan, Obese ZDF rats fermented resistant starch with effects on gut microbiota but no reduction in abdominal fat, *Mol. Nutr. Food Res.*, 2017, **61**, 1501025.

90 T. S. Nielsen, Z. Bendiks, B. Thomsen, M. E. Wright, P. K. Theil, B. L. Scherer and M. L. Marco, High-Amylose Maize, Potato, and Butyrylated Starch Modulate Large Intestinal Fermentation, Microbial Composition, and Oncogenic miRNA Expression in Rats Fed A High-Protein Meat Diet, *Int. J. Mol. Sci.*, 2019, **20**, 2137.

91 Y. Bai, Y. Li, T. Marion, Y. Tong, M. M. Zaiss, Z. Tang, Q. Zhang, Y. Liu and Y. Luo, Resistant starch intake alleviates collagen-induced arthritis in mice by modulating gut microbiota and promoting concomitant propionate production, *J. Autoimmun.*, 2021, **116**, 102564.

92 Y. Sun, L. Zhou, L. Fang, Y. Su and W. Zhu, Responses in colonic microbial community and gene expression of pigs to a long-term high resistant starch diet, *Front. Microbiol.*, 2015, **6**, 877.

93 Y. Sun, Y. Su and W. Zhu, Microbiome-Metabolome Responses in the Cecum and Colon of Pig to a High Resistant Starch Diet, *Front. Microbiol.*, 2016, **7**, 779.

94 O. C. Umu, J. A. Frank, J. U. Fangel, M. Oostindjer, C. S. da Silva, E. J. Bolhuis, G. Bosch, W. G. Willats, P. B. Pope and D. B. Diep, Resistant starch diet induces change in the swine microbiome and a predominance of beneficial bacterial populations, *Microbiome*, 2015, **3**, 16.

95 S.-J. Bang, E.-S. Lee, E.-J. Song, Y.-D. Nam, M.-J. Seo, H.-J. Kim, C.-S. Park, M. Y. Lim and D.-H. Seo, Effect of raw potato starch on the gut microbiome and metabolome in mice, *Int. J. Biol. Macromol.*, 2019, **133**, 37–43.

96 R. J. Calvert, M. Otsuka and S. Satchithanandam, Consumption of raw potato starch alters intestinal function and colonic cell proliferation in the rat, *J. Nutr.*, 1989, **119**, 1610–1616.

97 L. M. Higgins, G. Frankel, I. Connerton, N. S. Goncalves, G. Dougan and T. T. MacDonald, Role of bacterial intimin in colonic hyperplasia and inflammation, *Science*, 1999, **285**, 588–591.

98 D. B. Coulon, R. Page, A. M. Raggio, J. Guice, B. Marx, V. Gourineni, M. L. Stewart and M. J. Keenan, Novel Resistant Starch Type 4 Products of Different Starch Origins, Production Methods, and Amounts Are Not Equally Fermented when Fed to Sprague-Dawley Rats, *Mol. Nutr. Food Res.*, 2020, **64**, e1900901.

99 H. Israelson, A. Vedsted-Jakobsen, L. Zhu, A. Gagnaire, A. von Münchow, N. Polakovicova, A. H. Valente, A. Raza, A. I. S. Andersen-Civil, J. E. Olsen, L. J. Myhill, P. Geldhof and A. R. Williams, Diet composition drives tissue-specific intensity of murine enteric infections, *mBio*, 2024, **15**, e0260323.

100 H. Shiratori, K. M. Hattori, K. Nakata, T. Okawa, S. Komiyama, Y. Kinashi, Y. Kabumoto, Y. Kaneko, M. Nagai, T. Shindo, N. Moritoki, Y. I. Kawamura, T. Dohi, D. Takahashi, S. Kimura and K. Hase, A purified diet affects intestinal epithelial proliferation and barrier functions through gut microbial alterations, *Int. Immunol.*, 2024, **36**, 223–240.

101 B. P. Willing, A. Vacharaksa, M. Croxen, T. Thanachayanont and B. B. Finlay, Altering host resistance to infections through microbial transplantation, *PLoS One*, 2011, **6**, e26988.

102 S. Alavi, J. D. Mitchell, J. Y. Cho, R. Liu, J. C. Macbeth and A. Hsiao, Interpersonal Gut Microbiome Variation Drives Susceptibility and Resistance to Cholera Infection, *Cell*, 2020, **181**, 1533–1546.

103 S. M. Holmberg, R. H. Feeney, P. K. V. Prasoodanan, F. Puértolas-Balint, D. K. Singh, S. Wongkuna, L. Zandbergen, H. Hauner, B. Brandl, A. I. Nieminen, T. Skurk and B. O. Schroeder, The gut commensal Blautia maintains colonic mucus function under low-fiber consumption through secretion of short-chain fatty acids, *Nat. Commun.*, 2024, **15**, 3502.

104 B. Mao, W. Guo, S. Cui, Q. Zhang, J. Zhao, X. Tang and H. Zhang, Blautia producta displays potential probiotic properties against dextran sulfate sodium-induced colitis in mice, *Food Sci. Hum. Wellness*, 2024, **13**, 709–720.

105 H.-X. Guo, Z.-H. Ji, B.-B. Wang, J.-W. Ren, W. Gao and B. Yuan, Walnut peptide ameliorates DSS-induced colitis in mice by inhibiting inflammation and modulating gut microbiota, *J. Funct. Foods*, 2024, **119**, 106344.

106 D. Carson, R. Barry, E. G. D. Hopkins, T. I. Roumeliotis, D. García-Weber, C. Mullineaux-Sanders, E. Elinav, C. Arrieumerlou, J. S. Choudhary and G. Frankel, Citrobacter rodentium induces rapid and unique metabolic and inflammatory responses in mice suffering from severe disease, *Cell. Microbiol.*, 2020, **22**, e13126.

107 E. G. D. Hopkins, T. I. Roumeliotis, C. Mullineaux-Sanders, J. S. Choudhary and G. Frankel, Intestinal Epithelial Cells and the Microbiome Undergo Swift Reprogramming at the Inception of Colonic Citrobacter rodentium Infection, *mBio*, 2019, **10**, e00062–e00019.

108 Y. A. Yap, K. H. McLeod, C. I. McKenzie, P. G. Gavin, M. Davalos-Salas, J. L. Richards, R. J. Moore, T. J. Lockett, J. M. Clarke, V. V. Eng, J. S. Pearson, E. E. Hamilton-Williams, C. R. Mackay and E. Mariño, An acetate-yielding diet imprints an immune and anti-microbial programme against enteric infection, *Clin. Transl. Immunol.*, 2021, **10**, e1233.

109 N. Nakanishi, K. Tashiro, S. Kuhara, T. Hayashi, N. Sugimoto and T. Tobe, Regulation of virulence by butyrate sensing in enterohaemorrhagic Escherichia coli, *Microbiology*, 2009, **155**, 521–530.

110 G. C. J. Abell, C. M. Cooke, C. N. Bennett, M. A. Conlon and A. L. McOrist, Phylotypes related to Ruminococcus bromii are abundant in the large bowel of humans and increase in response to a diet high in resistant starch, *FEMS Microbiol. Ecol.*, 2008, **66**, 505–515.

111 M. M. Curtis, Z. Hu, C. Klimko, S. Narayanan, R. Deberardinis and V. Sperandio, The gut commensal Bacteroides thetaiotaomicron exacerbates enteric infec-

tion through modification of the metabolic landscape, *Cell Host Microbe*, 2014, **16**, 759–769.

112 N. Kamada, Y. G. Kim, H. P. Sham, B. A. Vallance, J. L. Puente, E. C. Martens and G. Nunez, Regulated virulence controls the ability of a pathogen to compete with the gut microbiota, *Science*, 2012, **336**, 1325–1329.

113 D. E. Chang, D. J. Smalley, D. L. Tucker, M. P. Leatham, W. E. Norris, S. J. Stevenson, A. B. Anderson, J. E. Grissom, D. C. Laux, P. S. Cohen and T. Conway, Carbon nutrition of Escherichia coli in the mouse intestine, *Proc. Natl. Acad. Sci. U. S. A.*, 2004, **101**, 7427–7432.

114 A. J. Fabich, S. A. Jones, F. Z. Chowdhury, A. Cernosek, A. Anderson, D. Smalley, J. W. McHargue, G. A. Hightower, J. T. Smith, S. M. Autieri, M. P. Leatham, J. J. Lins, R. L. Allen, D. C. Laux, P. S. Cohen and T. Conway, Comparison of carbon nutrition for pathogenic and commensal Escherichia coli strains in the mouse intestine, *Infect. Immun.*, 2008, **76**, 1143–1152.

115 C. P. Simmons, N. S. Goncalves, M. Ghaem-Maghami, M. Bajaj-Elliott, S. Clare, B. Neves, G. Frankel, G. Dougan and T. T. MacDonald, Impaired resistance and enhanced pathology during infection with a noninvasive, attaching-effacing enteric bacterial pathogen, Citrobacter rodentium, in mice lacking IL-12 or IFN-gamma, *J. Immunol.*, 2002, **168**, 1804–1812.

116 Y. Zheng, P. A. Valdez, D. M. Danilenko, Y. Hu, S. M. Sa, Q. Gong, A. R. Abbas, Z. Modrusan, N. Ghilardi, F. J. de Sauvage and W. Ouyang, Interleukin-22 mediates early host defense against attaching and effacing bacterial pathogens, *Nat. Med.*, 2008, **14**, 282–289.

117 R. M. Locksley, Nine lives: plasticity among T helper cell subsets, *J. Exp. Med.*, 2009, **206**, 1643–1646.

118 S. Commins, J. W. Steinke and L. Borish, The extended IL-10 superfamily: IL-10, IL-19, IL-20, IL-22, IL-24, IL-26, IL-28, and IL-29, *J. Allergy Clin. Immunol.*, 2008, **121**, 1108–1111.

119 D. M. Mosser and X. Zhang, Interleukin-10: new perspectives on an old cytokine, *Immunol. Rev.*, 2008, **226**, 205–218.

120 K. Wolk, S. Kunz, E. Witte, M. Friedrich, K. Asadullah and R. Sabat, IL-22 increases the innate immunity of tissues, *Immunity*, 2004, **21**, 241–254.

121 N. J. Wilson, K. Boniface, J. R. Chan, B. S. McKenzie, W. M. Blumenschein, J. D. Mattson, B. Basham, K. Smith, T. Chen, F. Morel, J. C. Lecron, R. A. Kastelein, D. J. Cua, T. K. McClanahan, E. P. Bowman and R. de Waal Malefyt, Development, cytokine profile and function of human interleukin 17-producing helper T cells, *Nat. Immunol.*, 2007, **8**, 950–957.

122 S. V. Kotenko, L. S. Izotova, O. V. Mirochnitchenko, E. Esterova, H. Dickensheets, R. P. Donnelly and S. Pestka, Identification, cloning, and characterization of a novel soluble receptor that binds IL-22 and neutralizes its activity, *J. Immunol.*, 2001, **166**, 7096–7103.

123 F. Liao, R. L. Rabin, J. R. Yannelli, L. G. Koniaris, P. Vanguri and J. M. Farber, Human Mig chemokine: biochemical and functional characterization, *J. Exp. Med.*, 1995, **182**, 1301–1314.

124 M. E. Spehlmann, S. M. Dann, P. Hruz, E. Hanson, D. F. McCole and L. Eckmann, CXCR2-dependent mucosal neutrophil influx protects against colitis-associated diarrhea caused by an attaching/effacing lesion-forming bacterial pathogen, *J. Immunol.*, 2009, **183**, 3332–3343.

125 S. A. Reid-Yu, B. R. Tuinema, C. N. Small, L. Xing and B. K. Coombes, CXCL9 contributes to antimicrobial protection of the gut during citrobacter rodentium infection independent of chemokine-receptor signaling, *PLoS Pathog.*, 2015, **11**, e1004648.

126 M. Okda, S. Spina, B. S. Fakhr and R. W. Carroll, The Antimicrobial Effects of Nitric Oxide: A Narrative Review, *Nitric Oxide*, 2025, **155**, 20.

127 W. Niedbala, J. C. Alves-Filho, S. Y. Fukada, S. M. Vieira, A. Mitani, F. Sonego, A. Mirchandani, D. C. Nascimento, F. Q. Cunha and F. Y. Liew, Regulation of type 17 helper T-cell function by nitric oxide during inflammation, *Proc. Natl. Acad. Sci. U. S. A.*, 2011, **108**, 9220–9225.

128 Y. Jianjun, R. Zhang, G. Lu, Y. Shen, L. Peng, C. Zhu, M. Cui, W. Wang, P. Arnaboldi, M. Tang, M. Gupta, C. F. Qi, P. Jayaraman, H. Zhu, B. Jiang, S. H. Chen, J. C. He, A. T. Ting, M. M. Zhou, V. K. Kuchroo, H. C. Morse 3rd, K. Ozato, A. G. Sikora and H. Xiong, T cell–derived inducible nitric oxide synthase switches off Th17 cell differentiation, *J. Exp. Med.*, 2013, **210**, 1447–1462.

129 T. Macleod, J. S. Ainscough, C. Hesse, S. Konzok, A. Braun, A. L. Buhl, J. Wenzel, P. Bowyer, Y. Terao, S. Herrick, M. Wittmann and M. Stacey, The Proinflammatory Cytokine IL-36γ Is a Global Discriminator of Harmless Microbes and Invasive Pathogens within Epithelial Tissues, *Cell Rep.*, 2020, **33**, 108515.

130 F. Colotta, F. Re, M. Muzio, R. Bertini, N. Polentarutti, M. Sironi, J. G. Giri, S. K. Dower, J. E. Sims and A. Mantovani, Interleukin-1 type II receptor: a decoy target for IL-1 that is regulated by IL-4, *Science*, 1993, **261**, 472–475.

131 D. Supino, L. Minute, A. Mariancini, F. Riva, E. Magrini and C. Garlanda, Negative Regulation of the IL-1 System by IL-1R2 and IL-1R8: Relevance in Pathophysiology and Disease, *Front. Immunol.*, 2022, **13**, 804641.

132 B. Chassaing, G. Srinivasan, M. A. Delgado, A. N. Young, A. T. Gewirtz and M. Vijay-Kumar, Fecal lipocalin 2, a sensitive and broadly dynamic non-invasive biomarker for intestinal inflammation, *PLoS One*, 2012, **7**, e44328.

133 W. G. W. Pathirana, S. P. Chubb, M. J. Gillett and S. D. Vasikaran, Faecal Calprotectin, *Clin. Biochem. Rev.*, 2018, **39**, 77–90.

134 J. Qiu, J. J. Heller, X. Guo, Z. M. Chen, K. Fish, Y. X. Fu and L. Zhou, The aryl hydrocarbon receptor regulates gut immunity through modulation of innate lymphoid cells, *Immunity*, 2012, **36**, 92–104.

135 C. R. Chiaro, R. D. Patel, C. B. Marcus and G. H. Perdew, Evidence for an aryl hydrocarbon receptor-mediated cyto-

chrome p450 autoregulatory pathway, *Mol. Pharmacol.*, 2007, **72**, 1369–1379.

136 S. Ke, A. B. Rabson, J. F. Germino, M. A. Gallo and Y. Tian, Mechanism of suppression of cytochrome P-450 1A1 expression by tumor necrosis factor-alpha and lipopolysaccharide, *J. Biol. Chem.*, 2001, **276**, 39638–39644.

137 I. A. Murray, R. G. Nichols, L. Zhang, A. D. Patterson and G. H. Perdew, Expression of the aryl hydrocarbon receptor contributes to the establishment of intestinal microbial community structure in mice, *Sci. Rep.*, 2016, **6**, 33969.

138 Y. Li, S. Innocentin, D. R. Withers, N. A. Roberts, A. R. Gallagher, E. F. Grigorieva, C. Wilhelm and M. Veldhoen, Exogenous stimuli maintain intraepithelial lymphocytes via aryl hydrocarbon receptor activation, *Cell*, 2011, **147**, 629–640.

139 C. N. Berger, V. F. Crepin, T. I. Roumeliotis, J. C. Wright, D. Carson, M. Pevsner-Fischer, R. C. D. Furniss, G. Dougan, M. Dori-Bachash, L. Yu, A. Clements, J. W. Collins, E. Elinav, G. J. Larrouy-Maumus, J. S. Choudhary and G. Frankel, Citrobacter rodentium Subverts ATP Flux and Cholesterol Homeostasis in Intestinal Epithelial Cells In Vivo, *Cell Metab.*, 2017, **26**, 738–752.

140 M. Peng, N. Yin, S. Chhangawala, K. Xu, C. S. Leslie and M. O. Li, Aerobic glycolysis promotes T helper 1 cell differentiation through an epigenetic mechanism, *Science*, 2016, **354**, 481–484.

141 L. Araujo, P. Khim, H. Mkhikian, C. L. Mortales and M. Demetriou, Glycolysis and glutaminolysis cooperatively control T cell function by limiting metabolite supply to N-glycosylation, *eLife*, 2017, **6**, e21330.

142 Z. Zha, Y. Lv, H. Tang, T. Li, Y. Miao, J. Cheng, G. Wang, Y. Tan, Y. Zhu, X. Xing, K. Ding, Y. Wang and H. Yin, An orally administered butyrate-releasing xylan derivative reduces inflammation in dextran sulphate sodium-induced murine colitis, *Int. J. Biol. Macromol.*, 2020, **156**, 1217–1233.

143 Y. L. Huang, J. M. Zheng, Z. Y. Shi, H. H. Chen, X. T. Wang and F. B. Kong, Inflammatory proteins may mediate the causal relationship between gut microbiota and inflammatory bowel disease: A mediation and multivariable Mendelian randomization study, *Medicine*, 2024, **103**, e38551.

144 L. Bordoni, R. Gabbianelli, D. Fedeli, D. Fiorini, I. Bergheim, C. J. Jin, L. Marinelli, A. Di Stefano and C. Nasuti, Positive effect of an electrolyzed reduced water on gut permeability, fecal microbiota and liver in an animal model of Parkinson's disease, *PLoS One*, 2019, **14**, e0223238.

145 S. Solaymani-Mohammadi and J. A. Berzofsky, Interleukin 21 collaborates with interferon-gamma for the optimal expression of interferon-stimulated genes and enhances protection against enteric microbial infection, *PLoS Pathog.*, 2019, **15**, e1007614.